Development of a switchable, tunable surfactant drag reducing solution for application in recirculating heat transport systems

A Thesis

Presented in Partial Fulfillment of the Requirements for Bachelors of Science Graduation with Honors Distinction in Chemical Engineering, The Ohio State University

By

Lucas Watson

Department of Chemical and Biomolecular Engineering

The Ohio State University

2018

Honor's Examination Committee:

Jacques Zakin (Deceased), Advisor

Andrew Maxson, Advisor

Kurt Koelling

© Copyright by

Lucas Watson

2018

Abstract

Surfactant drag reduction is a flow phenomenon by which as little as a few parts per million of certain chemical additives can reduce the turbulent pressure loss by over 80%. Various drag reducing additives exist; however, surfactant drag reducing additives are unique in their ability to rapidly reassemble after periods of high shear, making them particularly useful in recirculating systems. Such recirculating systems include district heating or cooling systems.

One intrinsic limitation of drag reducing solutions is their reduced heat transfer ability. This limits their usefulness as heat transfer fluids. For this reason, various methods of increasing heat transfer in drag reducing fluids have been developed. All of these prior methods, unfortunately, act on not only the drag reducing structures, but also the bulk solvent. Surfactant drag reducing fluids are also unique in that due to their self assembled nature, they have the potential to be "switched" on or off. This is done by modifying the thermodynamic equilibrium structure of surfactant micelles from drag reducing(heat transfer reducing) structures to non-drag reducing (non-heat transfer reducing) structures, and back to drag reducing structures.

This has been done with some success by modifying the chemical composition; however, whatever chemical composition changes that are made need to be reversed. In the case of pH adjustment, for example, salts accumulate in the system. The most desirable case would be a self assembled (shear stable) drag reducing solution that can

be switched (for excellent heat transfer) by modifying only the drag reducing nanostructures, and that switch is done only using stimuli intrinsic to a district heating or cooling system (flow rate or temperature).

In this study, a surfactant drag reducing system was developed showing extreme responsiveness to very small changes in temperature and flow rate. Furthmore, the flow rate "switch" could be shifted with temperature and vice versa. These shifts were correlated with shear viscosity data. These shifts were compared with Cryo-TEM images, prior work, and predictions from thermodynamics. The switch developed could be used to understand the structures that cause drag reduction.

To Prof. Zakin

Table of Contents

Page

List of Figures

Chapter 1: Introduction

1.1 Drag Reduction

Drag reduction is a phenomenon by which modification of a flow causes a reduction in the turbulent pressure loss. Drag reducing phenomena can be divided into two categories - drag reduction by surface modification and by additives. Examples of drag reduction by surface modification include superhydrophobicity [23] and surface texturing [19]. Examples of drag reduction by additives include paper pulp [18], high molecular weight polymers [74], aluminum disoaps [53], and surfactant micelles [78]. Polymer drag reducing additives have found many applications including the oil pipe lines [6], fire hoses [17], and undercapacity storm sewers [21]. All of these aforementioned applications are "once through"' systems. This is because polymer drag reducing additives are permanently degraded after periods of high shear (i.e. pumps, constrictions, etc.) and lose their drag reducing effectiveness [31]. Therefore, polymer drag reducing additives must be constantly replenished.

1.2 Surfactant Drag Reduction

To avoid this issue, various surfactant drag reducing additives have been developed. Surfactants, or surface active agents, self-assemble into a variety of morphologies, some of which are drag reducing. These self-assembled structures are able to reform and regain drag reducing effectiveness after periods of high shear [78] [57]. This makes surfactant drag reducing additives suitable for application to recirculating systems.

1.3 Surfactant Drag Reducing Additives in Recirculating Heat Transport Systems

Recirculating heat transport systems are widely used throughout industry for both heating and cooling. These systems have numerous advantages over dispersed, independent heating or cooling units. A centralized heating or cooling unit has lower maintenance cost, for the same required output a larger heating or cooling unit will cost less than many smaller units summed together, and waste heat from other processes (eg coal combustion for power generation) can be utilized by the surrounding community. One apparent limitation of these systems is the pumping energy requirement to move the working fluid over such long distances. Surfactant drag reducing additives have been sucessfully been used in district heating systems to reduce the turbulent pressure loss and thus the pumping energy requirments [33] [45]. However, surfactant drag reducing additives are still not effective in some systems due to their reduced convective heat transport, which is always higher than the reduction in drag [1].

1.4 Project Scope

In the following chapters, a review of surfactant micelles, their solutions, and current methods of heat transfer enhancement in micelle solutions will be presented. A novel "switchable" surfactant drag reducing solution and its development will be described. The experimental techniques to characterize the drag reduction, heat transfer, rheological, and structural properties of this novel solution will be illustrated. Lastly, correlations will be presented between the drag reduction/heat transfer, rheological, structural, and thermodynamic trends.

Chapter 2: Literature Review

2.1 Surfactant Micelles

2.1.1 Surfactants

Surfactants, or surface active agents, are ampiphillic molecules consisting of a polar head group and a nonpolar tail. Surfactants can be classified by their headgroup charge as either cationic, anionic, nonionic, or zwitterionic [12]. Furthermore, surfactants can be classified according to the structure of their skeleton as linear, gemini, or bolaform [79]. Surfactants are often produced from natural fats, and thus many commercial surfactants posses a wide distribution of tail lengths.

The thermodynamics of surfactants in solution can be divided into four fundamental processes: dissolution of the surfactant, aggregation of surfactants, adsorption of surfactants at interfaces, and transport of surfactants from the bulk to an interface. Surfactants in aqueous solution are only sparingly soluble due to the large hydrophobic tail. Upon addition of surfactants to water, they will dissolve, and then some amount of the surfactants will migrate to the interfaces. The surfactants arrange themselves such that the polar head group is in contact with the water while the nonpolar tail is interacting with the interface. This leads to a surface tension lowering effect. Upon further increase in concentration, surfacatants will spontaneously self assemble into micelles [52].

2.1.2 CMC

Various physical properties can be used to measure the concentration of surfactants in aqueous solution. These include conductivity, turbidity, and surface tension. If one of these properties, such as conductivity, is plotted vs surfactant concentration, conductivity will increase linearly until a certain concentration. Above that concentration, there is an inflection point, and then conductivity will increase linearly once again but with a different slope. The intersection of these two straight lines is the critical micelle concentration (CMC) [52] [78][27]. It can be shown that below the CMC, the monomer concentration is equal to the total surfactant concentration[52]. Above the CMC, the monomer surfactant concentration varies very little, and any additional surfactant added goes into the micelles [27].

2.1.3 Micelle Formation

Once above the CMC, surfactant micelles form. There are two models for the formation of surfactant micelles - micellezation as a chemical rection and micellezation as a phase equilbrium [27][52].

Micellezation as a Chemical Reaction

Micelle formation as a chemical reaction can be expressed as $\mathrm{nS} \overset{\mathrm{K_n}}{\rightleftharpoons} \mathrm{M_n}$ where n is the aggregation number (surfactant molecules per micelle), K_n is the rate constant for formation of a micelle of aggregation number n, S is the surfactant concentration, and M_n is the concentration of micelles of aggregation number n [52] [27]. Treating micelle formation as a chemical reaction is the more rigorous method at low concentrations [52]. However, due to the large aggregation numbers at higher concentrations, one cannot think of a micelle as a chemical species. Furthermore, due to

the polydispersity of surfactant micelles, the number of rate constants needed to fully describe the system is unrealistic. Lastly, this mass action model correctly predicts an increasing micelle concentration at higher surfactant concentrations, but it fails to predict the very large aggregation numbers that occur in most aqueous systems. For this reason, at increasing concentrations, it is more common to model surfactant micelles as a pseduophase [52][27].

Micellezation as a Phase Equilibrium

Thinking of micelles as a separate pseudophase, the micelle size distribution and micelle geometry at equilibrium are such that the difference in chemical potential of a surfactant in solution and in a micelle in minimized. In general, the enthalpic component of micelle formation can be both positive or negative, while the main driving force for micelle formation is the hydrophobic effect.

The hydrophobic effect, colloquially "like dissolve like", is the large and positive change in entropy when oil and water separate. The hydrophobic tail of a surfactant, when dissolved in water, can be thought of as causing a hole in the hydrogen bonding of the surrounding water molecules. When the hydrophobic tail is segregated to the core of the micelle, there is a slight decrease in entropy from constraining the tail; however, the increase in water-water interactions causes a much larger increase in entropy, driving micelle formation [27].

However, exactly how surfactants arrange into micelles is more complicated. The various contributions to the free energy of a micelle pseudophase can be divided into the transfer free energy, deformation free energy, aggregate core-water interfacial free energy, head group steric interactions, and head group ionic interactions. Other, less

commonly considered interactions exist such as dipole-dipole interactions in zwitterionic surfactant micelles, nonideal mixing of unequal tail lengths, packing of unequal sized headgroups, etc. [54] [55]. The net effects of these contributions to the free energy will be described in the next section on micelle structure.

The transfer free energy is the energy required to transfer a surfactant's tail from the bulk solution to the interior of a micelle. This can be estimated by modeling the core of the micelle as liquid hydrocarbon (of equivalent composition to the surfactant tail), and then using data for the solubility of the hydrocarbon in water and in itself. This is a strong function of hydrocarbon tail length and a function of temperature.

The deformation free energy is the energy required to pack the tails together inside the micelle. This is a linear function of hydrocarbon tail length and a weak function of temperature (due to increased thermal motion). Furthermore, double bonds and bulky groups that make the tail more stiff also contribute to this term. This term is a function of micelle morphology. This term can be estimated from knowledge of the tail group's dimensions and knowledge of the micelle morphology.

The aggregate-core interfacial free energy is the free energy of oily core that is left unshielded from the water. This can be estimated from surface tension data and is a function of temperature, tail size, and the size of the surfactant head group when incorporated into the micelle.

The head group steric energy is caused by the steric repulsions between surfactant head groups when packed into a micelle. This is a function of head group size.

The head group ionic free energy is caused by the ionic repulsions of the like charged head groups in the surfactant micelle. This is a complicated function of

temperature (dehydration of counterions, increase thermal motion of the counterions), head group size and type, ionic strength and concentration of the counterions, permitivity of solvent, micelle morphology, and more.

In total, surfactant micelle parameters can be predicted from the sum of the contributions to the free energy, and then minimizing the difference in chemical potential between a surfactant in the singly dispersed state and in a micelle, $\Delta\mu_g$. This is expressed as

$$\Delta\mu_g = \Delta\mu_{transfer} + \Delta\mu_{deformation} + \Delta\mu_{interfacial} + \Delta\mu_{steric} + \Delta\mu_{ionic} \tag{2.1}$$

2.1.4 Micelle Structure

The structure of surfactant micelle can be compactly described by its packing parameter, P. The packing parameter is defined as

$$P = \frac{V}{a_e l} \tag{2.2}$$

where V is the volume of the hydrophobic chain, a_e is the area per molecule at the equilibrium aggregate interface, and l is the length of the hydrophobic chain. The morphology of the surfactant micelle varies with packing parameter:

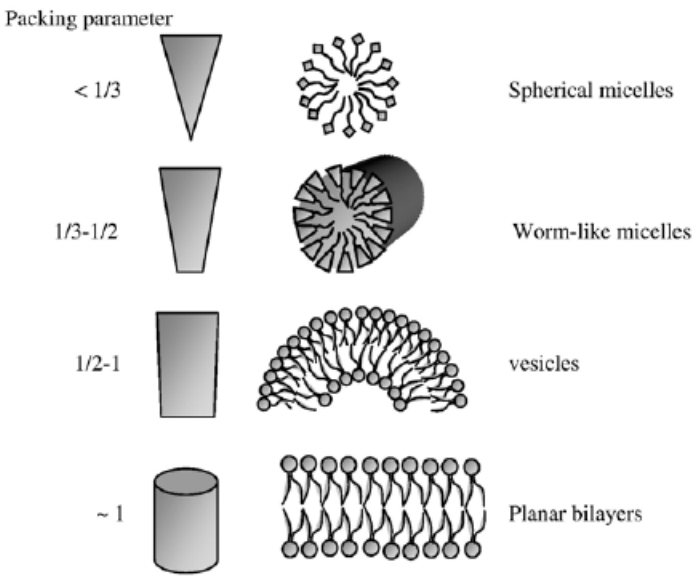

Figure 2.1: Micelle morphology with packing parameter [70]

Missing from the above figure is network micelles, which are intermediate between vesicles and wormlike micelles. Networks form to reduce the number of endcaps [25].

The cumulative effects of temperature and counterion concentration on micelle structure predicted by thermodynamics(discussed above) are as follows: increasing the temperature leads to a net decrease in the in the packing parameter (for ionic surfactants), increasing counterion concentration leads to a net increase in the packing parameter [55] [54] [11]. The exact amount the packing parameter changes with these variables is complicated and varies between different surfactant-counterion combinations.

One particular variation worth mentioning is the difference in how the counterions bind to the micelles. Hydrotrpoic counterions(counterion with both polar and non-polar parts) embed in different orientations and to different depths. This can

lead to a significant difference in the headgroup charge neutralization [77]. Many commonly used hydrotropic counterions are substituted benzenes. It has been found that hydrophobic substituients(eg chloro groups) make micellezation more exothermic [8]. Counterions that deeply penetrate the micelle headgroup plane greatly promote micelle growth [46]. Counterions with hydrophobic groups oriented toward the hydrophobic core and hydrophillic groups oriented toward the micelle surface bind more strongly [68]. More hydrophobic counterions, such as chloro substitiuted benzenes, bind more strongly due to their lower solubility [26]. The ability of a counterion to bind to the micelle strongly effects the micelle head group area[56]. The strong binding of hydrophobic counterions leads to vesicles forming at relatively low counterion ratios[26]. Increasing hydrophoboicty of the counterion is analagous to increasing salt concentration [25].

Besides the packing parameter, the length and flexibility of micelles have dramatic effect on the rheological properties of their solutions [78]. It is often stated as fact in the literature that flow aligned wormlike micelles are the cause of drag reduction [37][4]. Shorter micelles require more deformation to align with flow [73], and below a certain micelle length, they are no longer drag reducing[77]. The viscosity of wormlike micelle solutions varies very strongly with micelle length [78].

2.2 Surfactant Drag Reduction

Drag reduction is defined as the fractional reduction in the fanning friction factor

$$DR = \frac{f_{solvent} - f_{DR}}{f_{solvent}} \tag{2.3}$$

Typically, %DR is plotted vs solvent Reynolds number (Reynolds number calculated using the density and viscosity of the solvent at experimental conditions). This decision is a matter of convention to avoid addressing the non-newtonian viscosity of surfactant solutions. Co-solvent‘s have been successfully used with surfactant drag reducing solutions. For example, Zhang et al found that significant drag reduction could be achieved down to 0 degC with up to 28% ethylene glycol in water with ethoxylated surfactants [81].

Drag reduction vs solvent Reynolds number curves can be shifted to higher flow rates with increasing counterion concentration [44][40]. With only a few exceptions, drag reduction curves get shifted to higher Reynolds number with increasing temperature. This can be seen in [41][40][42][81][68][43]. This can be reasoned as the shortening of micelles with increasing temperature requiring more shear to algin with flow.

2.3 Surfactant Micelle Rheology

2.3.1 Time-Dependence

Surfactant micelle solutions show various time dependent rheological effects. The most often of these discusessed is shear induced structure(SIS). SIS has been hypothesized to be giant wormlike micelles formed by end to end collision, fusion, and growth of shorter rodlike micelles [73][38]. The growth of SIS can lead to massive wormlike micelles, not observed in the quiescent state. There is even one report of SIS being visible with the naked eye [72].

Hu and Matthys have published several papers investigating the build up and decays of SIS. They found that at a steady shear rate, there is an induction time

before SIS is observed. This induction time varies with rheometer geometry (cone and plate, parallel plate, concentric cylinder). The induction time also varies with parallel plate gap and cone and plate radius. The induction time decreases with increasing shear rate. Interestingly, the shear does not have to be in a constant direction. Hu and Matthys conducted an experiment with the shear alternating clockwise and counter-clockwise direction. In this experiment, SIS growth was still observed after an induction time. Lastly, they found that after a very high preshear (2000/s) intended to fully shear degrade any SIS structures, the induction time for SIS was shorter than starting from quiscent. This suggests that SIS fragments were still present; however, they were not large enough to significantly effect rheological properties [28]. A similar effect can be seen in drag reduction data, as discussed in section 2.5.2.

2.3.2 Morphological Effects

Viscoelasticity and shear thinning in polymer solutions is caused by the deformation and relaxation of polymer molecules, particularly entangled polymers [11]. Surfactant wormlike micelles have more complicated rheological behavior due to additional modes of stress relaxation including chain scission, recombination, monomor transfer, and node slip [11]. Wormlike micelles are viscoelastic due to worm-worm entanglements, similar to polymers [56]. Womrlike micelles are also shear thinning [40] [39]

At high enough counterion concentration, network micelles begin to form to reduce the number of end caps (the sharp radius of an end cap is an energetically unfavorable surfactant packing). These network structures have a lower viscosity due to an additional mode of stress relaxation - node slip. A branch in a network

micelle can slide more quickly than wormlike micelles can reptate past one another [13] [49] [34]. As salt is added, the zero shear viscosity goest through a maxium at the wormlike to brached micelle transtition [13]. Node slip also causes a reduction (or elimination) of viscoelasticity [77][40]. Branched micelles can transition to more viscoelastic wormlike micelles with adequate deformation [56].

Spherical micelles and vesicles typically have uninteresting, newtonian rheological behavior [11]. However, vesicles have the potential to transition under shear to network or branched wormlike micelles [77] [26] [83] [39].

2.3.3 Flow-Imaging Techniques

Mendes et al studied morphological transitions of an ionic surfactant-counterion combination using Rheo-Small Angle Neutron Scattering (Rheo-SANS). Mendes et al observed that there is qualitatively an interchability of temperature, counterion concentration, and deformation rate on the structure of micelles in a couette flow [50]. The temperature and counterion trends for an ionic surfactant predicted from thermodynamics [55] [54] match the temperature and counterion trends observed by Mendes et al. The trends observed by Mendes et all are summarized in the following figure, which was adapted from Stuart [70] by adding annotations that show the trends in morphology with packing parameter. The effect of shear rate on packing parameter is consistent with prior Rheo-SANS results [7].

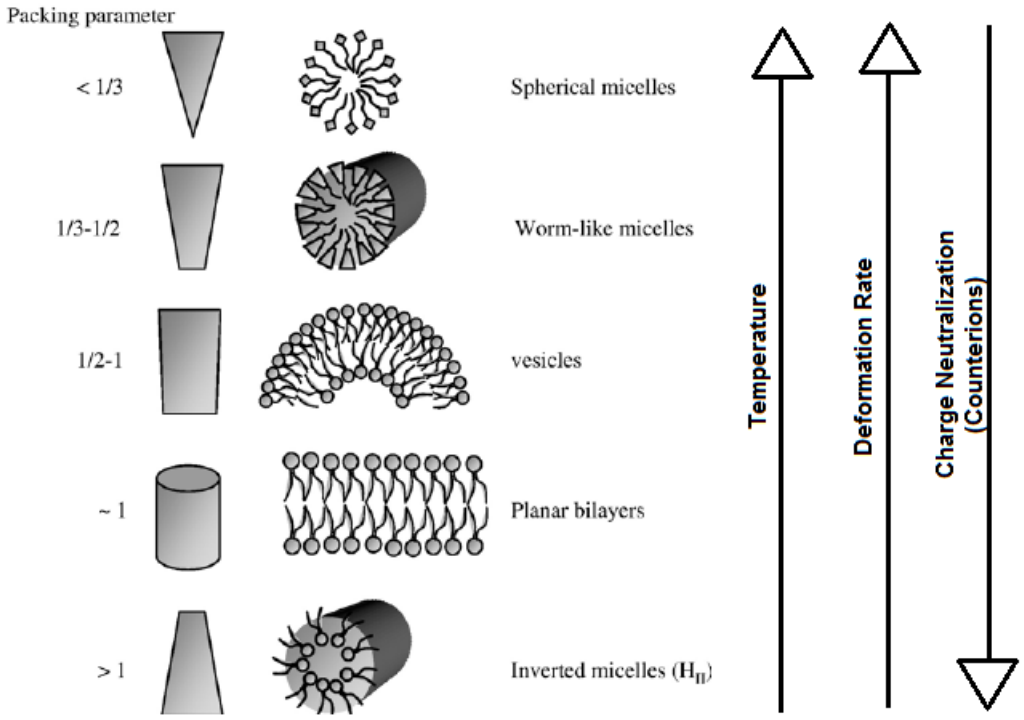

Figure 2.2: Packing parameter trends observed by Mendes et al [50]. Annotated and adapted from Stuart [70].

Rheo SANS data has also shown flow alignment of micelles in shear [24]. Freeze fracture microscopy experiments after a shear have shown highly entangld and flow aligned structures (what the authors claimed to be SIS) on the size scale of microns [30].

Cryogenic Tunneling Electron Microscopy(Cryo-TEM) is a common way to image transient structures. Cryo-TEM involves blotting a sample on a support and quickly vitrifying it. This has been successfully used to make tentative confirmation of hypothesized structures [13] [82]. However, the shear from blotting can effect the observation.

2.4 Mechanism of Drag Reduction

Various theories have been proposed for the mechanism of drag reduction. Although there is no clear answer to which, if any of the mechanisms are correct, the following non-exhaustive review show a mixture of quantitative and qualitative agreement with experimental observations.

Drag reducing additives only show a reduction in pressure drop relative to a pure solvent when in the turbulent regime [37]. It has been shown that drag reducing additives have greatly reduced turbulent fluctuations [9][76]. These two statements lead to the following mechanism of drag reduction: the drag reducing structures suppress the generation of turbulent vorticies, resulting in a decrease in velocity fluctuations, and thus a reduction in kinetic energy being dissipated [37].

Along with suppressing turbulence, drag reducing additives modify the turbulent structure [35] [36] [29]. It appears that drag reducing solutions show a decreased correlation, or decoupling, of component turbulent fluctuations. This decoupling causes a reduction in the Reynolds shear stress, and thus a reduction in the drag coefficient [20].

Another hypothesized modification to the turbulent structure is the idea of stabilization of turbulent vorticies. Turbulent eddies are a composition of progressively smaller vortexes. Turbulent eddies diffuse energy by cascading kinetic energy down through the progressively smaller vorticies. When the Reynolds stress in turbulent flow is on a similar order as the elastic stress in a drag reducing solution, the aforementioned cascading process can be truncated, reducing the energy dissipated [37] [14] [69] [61].

It has also been speculated the elastic nanostructures in drag reduced flow absorb energy from small vortices in the form of elastic stress, and then, through convection, transport that energy to the larger-scaled vortices. This process greatly decreases the dissipation of turbulent kinetic energy and thus causing drag reduction [15] [75].

Lastly, it has been proposed that drag reduction is caused by an apparent slip near the wall. It is claimed that a shear induced "gel-like" phase occurs near the wall. When the wall shear stress becomes great enough, the gel can fracture leading to a slip effect, decreasing wall friction, and thus causing drag reduction [16].

2.5 Heat Transfer Enhancement in Drag Reduced Flows

The reduction in turbulence present in drag reduced flow (discussed in section 2.4) as well as a thickened sublaywer [63] cause a reduction the the convective heat transfer of the flow [78]. This is referred to has heat transfer reduction (HTR) and is defined as

$$HTR = \frac{h_{solvent} - h_{DR}}{h_{solvent}} \tag{2.4}$$

Heat transfer reduction is always higher than drag reduction [1]. To enhance heat transfer either the drag reducing structures can be destroyed, the structure of the flow changed (by modifying the geometry of the heat transfer surface), or the thermodynamic stability of the micelles can be altered temporarily. These approaches have been examined and the results of these investigations are described below.

2.5.1 Destruction of Surfactant Wormlike Micelle Structures

The direct method of enhancing the heat transfer ability of surfactant drag reducing solutions in shell and tube heat exchanges is by destroying their WLM nanostructures at the entrance to the exchanger so that the solution exhibits "water-like" heat transfer behavior while passing through all or most of the exchanger. The WLM structures then reassemble downstream so that drag reducing behavior is regained.

The effects of these techniques to destroy the micelle nanostructures to give heat transfer enhancement depends on their destruction effectiveness and also on the recovery time of the micelles, which can reform in seconds[57] causing the solution to become drag reducing again within the heat exchanger.

Both static mixers and honeycombs at the entrance to the heat exchanger were studied by Qi et al [57]. These are easy to install, with no moving parts, and so would be convenient to retrofit existing heat exchangers. In those experiments HTR at Reynolds numbers of 20,000 to 50,000 without the devices reached as high as 65%. The insertion of a honeycomb (Figure 2.3C) at the entrance had little effect on the heat transfer. However, with five elements of plastic Static Mixer B (Figure 2.3B) HTR was lowered to 40%. The static mixer, while moderately effective caused significant pressure losses thus reducing the advantage of using the drag reducing additive. See Section 2.5.3 for a discussion of metal Static Mixer A, which utilized a different mechanism of heat transfer enhancement.

Qi, et al [60] investigated the effect of exposing drag reducing solutions to ultrasonic energy radiation. This broke up the surfactant WLM nanostructures which reduced their turbulence inhibition effect and enhanced the solution's heat transfer ability. HTR was decreased to 24% from 82% with 300 seconds of ultrasonic exposure.

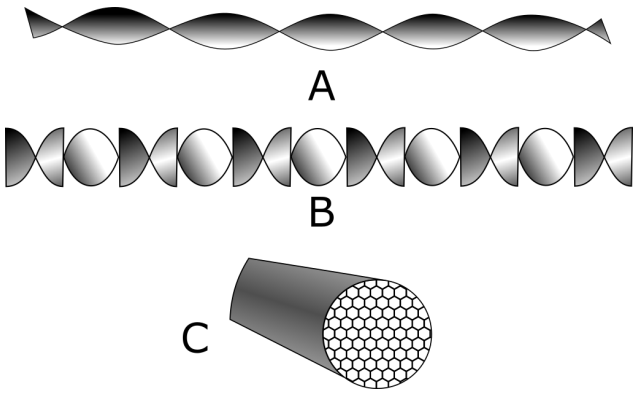

Figure 2.3: Previously studied static mixing devices [57]: A) twisted tape turbulator - "metal Static Mixer A", B) alternating helix mixer - "plastic Static Mixer B", C) honeycomb

While this technique was effective in enhancing heat transfer, the amount of energy required was large, and imparting such a large amount of energy for micelle breakup to a solution flowing at 1 meter /second or more is not practical.

2.5.2 Recovery after a destructive device

Gasljevic [22] and Suzuki [71] studied the recovery time of a drag reducing surfactant solution after a sudden contraction. A solution of 2300 ppm Ethoquad T13-50 and 2000 ppm NaSal was subjected to a pressure drop of over 5 bar by a throttling valve [**?**]. Downstream of the valve, pressure drop measurements were taken to determine the recovery of drag reduction. Drag reduction was not fully recovered after 1000 diameters downstream of the valve. Suzuki found a similar result in flow through a rectangular duct with a sudden expansion followed by a contraction from a duct size of 60 $\times$ 150 mm to a size of 20 $\times$ 50 mm [71]. It was found that between 1000 and 2000 hydraulic diameters were required for fully developed DR flow following the sudden contraction in the solution of 1000 ppm Ethoquad O/12 and 600 ppm NaSal

(1.5:1 counterion ratio). These are in contrast to the recovery time after the shear degradation devices, described earlier and tested by Qi that recovered after about 480 tube diameters [57].

With the nonionic surfactant SPE 95285, found that the recovery of drag reduction after a shear degradation device was only time based, independent of velocity [22]. But with cationic surfactant Ethoquad T13/50 and NaSal counterion, Matthys observed a recovery length below a critical pressure drop of 3.1 bar across the destructive mesh used. Above that critical pressure drop, it was not possible to measure the recovery time of the solution. Bellamy et al. claimed that the difference between the recovery time and recovery length observed was because below a certain stress, a degradation device destroys the shear induced structures, but not its constituent micelles [2].

Bewersdorff and Ohlendorf observed that in tube flow if a certain flow rate was exceeded, the high shear stress would result in complete loss of drag reduction [3]. Upon lowering the flow rate drag reduction was regained immediately, however the formation of the micelles in the solutions used (n-tetradecyltrimethylammonium salicylate and hexadecyltrimethylammonium salicylate) took on the order of 10^3 to 10^4 seconds. They also attributed this behavior to the destruction of superordered structures that cause drag reduction while leaving the individual micelles intact.

Hu and Matthys studied the redevelopment of the first normal stress difference (N_1) after a degrading preshear [28]. N_1 is an indicator of viscoelasticity, which is believed by many to be necessary for DR in surfactant solutions. With a solution of 5 mM tris (2-hydroxyethyl) tallowalkyl ammonium acetate and 5 mM NaSal it took 60 seconds at a shear rate of 100/s before the onset of N_1. Then, they presheared the solution for 50 seconds at a rate of 2000/s which was high enough to degrade the

solution, resulting in a zero value for N_1. Interestingly, when they lowered the shear rate sharply from 2000 to 100/s, the N_1 immediately begin to develop, without the 60 second induction time. They speculated that there existed some smaller micelle structures that survived the preshear but were not large enough to produce N_1, and upon lowering the shear rate larger structures reassembled much more quickly than the same sample without pre-shearing.

Qi reported that with a fixed flow rate at 55 °C the recovery length after a static mixer was 480 tube diameters (about 2.5 seconds) while at 60 °C the length was reduced to 420 diameters (about 2 seconds). This could be attributed to the smaller micelles present in ionic surfactant solutions at higher temperatures [47]. Smaller micelles are more able to rearrange themselves into SIS [3]. These results support the aforementioned recovery results that below a certain stress applied to the solution the recovery times are much quicker.

Although there are challenges in understanding and designing shear degradation devices, they are relatively simple to install. Other destructive methods such as pH adjustments or exposure to UV light are easier to quantify in terms of recovery, but can be more complicated to implement. These methods and others are discussed in the following sections.

2.5.3 Modification of Flow Structure

The other approach to enhancing heat transfer in DR solutions is to modify the wall boundary layer and/or to increase radial turbulence intensity and hence radial heat transport. The following approaches have shown moderate or significant heat transfer enhancement.

In a study by Kishimoto et al. [32], cooling of a cationic drag reducing surfactant solution in a concentric tube heat exchanger was enhanced by modifying the turbulent structure with spirally grooved inner tubes. A smooth inner tube and two grooved tubes with different pitches were compared. It was found that the flow velocity range in which drag reduction and heat transfer reduction occurred in both grooved tubes became significantly narrower than that of the smooth tube. The fluted tube with the greater pitch was found to have a lower heat transfer coefficient than water at all velocities tested; however, the heat transfer coefficient of the less pitched of the two grooved tubes in a linear velocity rate range of 1.5 to 2.0 m/s (compared to the typical DHC system operating range of 1.0 to 2.0 m/s) was found to exceed that of water in a smooth tube. The increase in heat transfer was correlated with the increased shear at the tube wall.

The use of a fluted tube heat exchanger to increase heat transfer in cooling of both a cationic surfactant solution (Ethoquad T-1350) and a zwitterionic/anionic surfactant solution (SPE98330) was investigated by Qi et al. [58]. The Nusselt number reported for the Ethoquad T13-50 solution in the fluted tube (Figure 2.4) was more than 1.2 times that of water in a smooth tube and the ratio of pressure drop of Ethoquad T13-50 solution in the fluted tube to that of water in a smooth tube of equivalent diameter varied from 2.6 to 3.5 from 50 °C to 55 °C. For the SPE98330 solution the heat transfer coefficient was at least 1.4 times that of water in a straight tube with only mild pressure drop penalty. It was suggested that the discrepancy between enhancement results between the two solutions was due to a weaker nanostructure in the SPE98330 solution, allowing shear degradation within the fluted tube.

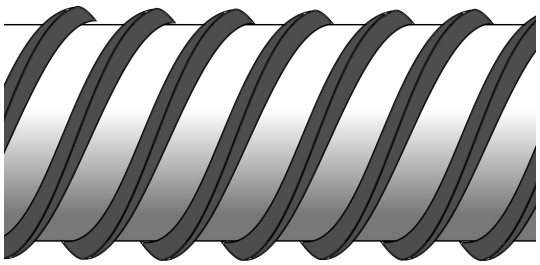

Figure 2.4: Fluted tube

While the pressure drop penalty for fluted tubes is relatively small [58], retrofitting a heat exchanger to employ grooved or fluted tubes would be impractical in many applications.

Since heat transfer is in the normal distance from the wall, Shi, et al. [67] studied the design of a high efficiency vortex (HEV) static mixer designed to promote radial turbulence intensity to enhance heat transfer but which had little effect on axial intensity, so as to minimize axial turbulence dissipation.

This static mixer concept involved forming tabs at the conduit wall inclined at a certain angle to the flow direction such that it enhances heat transfer between the wall and the flowing stream with the minimum amount of turbulent energy dissipation. Figure 2.5 illustrates the HEV design and Figure 2.6 shows the amount of heat transfer enhancement compared with static mixers.

Christensen and Zakin [10] reported that the reduction in heat transfer coefficient for a surfactant drag reducing solution in a chevron plate heat exchanger was 10-65% compared with up to 90+% for the same solution in a tube-in-tube heat exchanger. They attributed this to the chevron providing a pathway that inhibits wall boundary layer buildup. The economic viability of the use of such a plate heat exchanger in

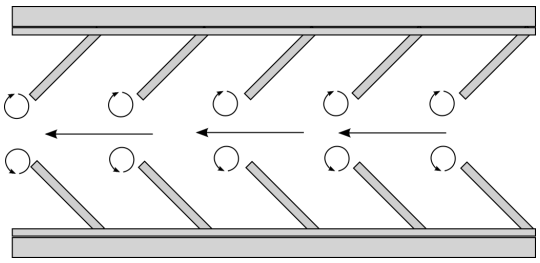

Figure 2.5: Design of HEV (not to scale)

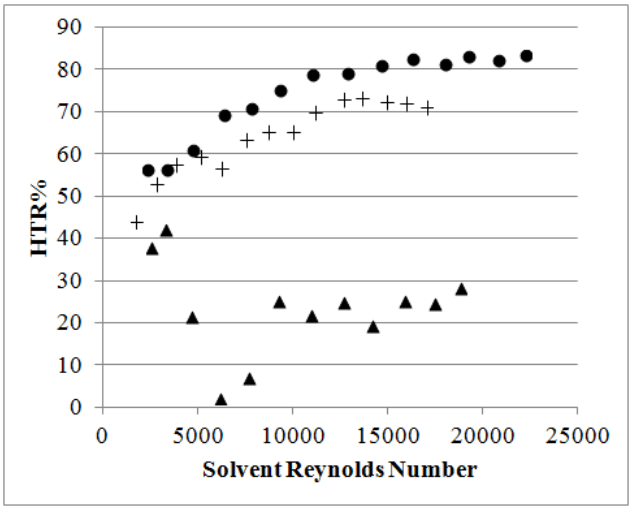

Figure 2.6: HTR vs Re for HEV (triangles), helical mixer (crosses), and no device (circles)

a particular application would depend on the capital and maintenance costs for this type of heat exchanger and on the suitability of the plate heat exchanger for the operating conditions.

Qi et al. [57] also tested the effectiveness of another type of static mixer to enhance heat transfer. A metal static mixer wih 15 elements designed to promote swirling flow (Figure 2.3A) inserted at the entrance to the heat exchanger decreased HTR% to less

than 40% but caused a pressure drop across the exchanger of 4x that of water flow with no device.

Our research group recently studied the effects of agitated heat exchangers on the heat transfer coefficients of a surfactant drag reducing solution. These devices were based on common designs of commercial scraped surface heat exchangers.

Using this method, there is no limit to the amount HTR% can be decreased, because the rotation rate of the agitator can be increased until HTR% reaches the desired level, at the cost of increasing power consumption. In this study, HTR% reached as low as -20%. By contrast, micelle destruction methods can only reach a minimum of 0% HTR.

The energy efficiency of the enhancement was better than most previously studied static devices, especially at high Reynolds numbers, and was comparable to the twisted tape turbulator studied by Qi et al. [57] [48].

2.5.4 Modification of Micelle Thermodynamic Stability

The minimum possible energy to have near water like heat transfer in a surfactant drag reducing solution would be the amount of energy required to make the nanostructures non-drag reducing without perturbing the solvent. To attempt to accomplish, various stimuli response or "smart" fluids have been developed.

Cationic surfactant drag reducing systems require an appropriate counterion to diffuse their positive charge facing the water phase and promote the growth of long wormlike micelles which modify the structure of the turbulent flow. If the molecular configuration of effective counterions can be altered at the entrance to a heat

exchanger to form an ineffective structure, the solution would lose its drag reduction character and show Newtonian properties with greatly enhanced heat transport.

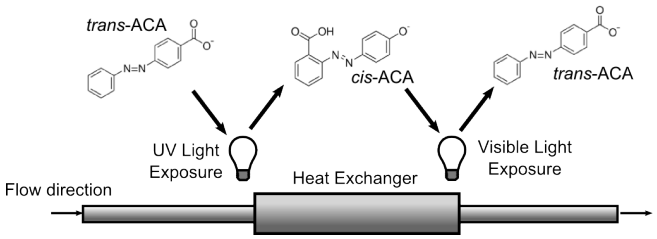

Figure 2.7: System for switchable drag reduction by photosensitive counterion

Shi, et al [65] studied light responsive counterions which were very effective as drag reducing counterions with cationic surfactants in *trans* configuration but not in the *cis* configuration. Thus if the drag reducing *trans* configuration counterion could be irradiated with UV light at the heat exchanger entrance and converted to the *cis* configuration, heat transfer would be enhanced in the exchanger. Irradiation with ordinary light would cause a reversal back to the drag reducing *trans* configuration. Figure 2.7 depicts this heat transfer enhancement method.

Despite the potential effectiveness of this approach, it requires more light energy to be absorbed by the solution at both ends of the heat exchanger than can be imparted to the flowing solution in a practical application.

pH responsive TLM systems have been developed by use of either pH sensitive surfactants or pH responsive counter ions. Such a chemical system could be used to promote heat transfer in drag reducing surfactant systems with local and reversible

pH adjustments by changing the geometry of the micelles [38] or flocculating the TLMs [66].

In the study by Shi et al. [66] using flocculation as a means to control drag reduction, it was shown that DR% could be changed between 80% and -20% over a pH range of approximately 2.0. Furthermore, their system was shown to be stable and reversible even after five pH cycles (from pH ~3 to ~10 and back).

Mizunuma [51] studied the heat transfer of viscoelastic and non-viscoelastic drag reducing surfactant solutions with excess counterions both in impinging jet and tube flow. The solutions studied were Ethoquad O/12 with sodium salicylate counterion in varying molar ratios ranging from 1:1 to 100:1. It was found that the effect of excess counterion ratio had little effect on heat transfer in tube flow; however, it was found that the reduction in heat transfer of the impinging jet disappeared with increased Re in the 1800 ppm 1:1 and 760 ppm 3:1 solutions. Also, the 400 ppm 30:1 and 400 ppm 100:1 solutions did not have any loss in heat transfer in the impinging jet flow. It was suggested that the disappearance in heat transfer reduction could be attributed to breakup of the micelles and that a combination of high counterion ratio and high shear at the heat exchanger entrance could lead to effective heat transfer enhancement of surfactant solutions.

Portions of this section were adapted from: Zakin, J. L., Maxson, A. J., Watson, L. J. (2016). "A Review of Studies of Heat Transfer Enhancement in Turbulent Drag Reducing Surfactant Solutions." *12th International Heat Transfer, Fluid Mechanics, and Thermodynamics Conference.*

2.6 Applications of Drag Reducing Additives

Drag reduction in turbulent flow of hydrocarbons containing small amounts of high polymer was first reported by Toms about 70 years ago. Previously, Mysels and his coworkers had observed similar behavior in solutions of aluminum disoaps. A few years later, drag reduction behavior was observed in dilute aqueous-surfactant solutions in which long wormlike micelles were present. In the late 1970's this phenomenon found its first commercial application when high molecular weight polymer was added to crude oil flowing through the 800-mile Alyeska pipeline. Crude flow was increased by about 25% with no additional pumps.

However high molecular weight polymers are not suited for use in recirculation systems because the high shear encountered in pumps breaks the primary chemical bonds within the polymer chains. The resulting low molecular weight polymer chain fragments are not efficient drag reducers, and they do not reassemble. On the other hand, surfactant micelles are held together by secondary forces and they reform (self-associate) very quickly after break-up in high shear regions (pumps). Thus, they are effective in recirculation systems.

District heating systems are widely used to heat buildings in urban locations in northern Europe and are also found in the US, Canada, Eastern Europe and other locales. These systems circulate hot water and exchange heat with each building thus relieving the buildings of the need for heat sources (furnaces) and the related investment, space, and maintenance required. They generally utilize cheap waste heat from nearby power plants to heat the circulating water. District cooling systems are utilized with the same advantages in some warm climate regions, particularly the United States and Japan. Applications in single-building air conditioning systems

have achieved 20-60% decreases in pumping power requirements [62]. Adding a drag reducing surfactant additive to the recirculating water could decrease pumping energy requirements of these systems by 50% or more. Various other applications of drag reducing additives include fire hoses [17], undercapcity storm sewers [21].

2.7 Summary

In summary, drag reducing surfactant solutions show a very diverse and complex range of morphological transitions. These transitions are controlled by temperature, counterion concentration, molecular structure, deformation, and more in very complicated and little understood ways. Attempts have been made to unite the thermodnamic predictions, rheology, and imaging techniques; however, little attempt has been made to unite these fields of study with drag reduction data. Furthermore, the mechanism of drag reduction is far from agreed upon. For these reasons, most current heat transfer enhancement techniques have exclusively relied on empiricism.

Chapter 3: Experimental Methods

3.1 Chemicals and Solution Preparation

Cetyltrimethylammounium cationic surfactant Arquad 16-50 acquired from Akzo Nobel with a known distribution of alkyl chain lengths was used. Specifically, C_{14} comprises approximately 12% of the alkyl chains, C_{15} 1%, C_{16} 75%, C_{17} 1% and C_{18} 11%. The surfactant is packaged as a concentrate with solvent content of 50 wt percent. The solvent is an aqueous ispopropanol mixture. The couterion, 3-chlorobenzoic acid was purchased in crystalline powder form from Fisher Scientific at greater than 99% purity. Solid NaOH pellets purchased from Mallinckrodt Chemical were added in equimolar ratio to the counterion.

Drag reduction and heat transfer reduction data was repeated on three different batches of the following solution. Arquad 16-50 concentrate was diluted with water to a concentration of 5 mM and a volume of 12 L. To this, 5 mM of the 3-chlorobenzoic acid was added as a counterion. The NaOH was added and the stock solution was mixed for 30 minutes using a high speed agitator. 2 L of this solution was used to rinse out the drag reducing flow loop. The remaining 10 liters were then added, and allowed to sit in the flow loop for 3 days before taking data.

At the end of each drag reduction experiment, a sample was saved for rheological testing. The 1.1:1 and 1.2:1 counterion ratio samples were made by adding counterion and NaOH to an amount of the 1:1 sample from the drag reducing system.

3.2 Drag Reduction Measurement

All tests were performed in a recirculating flow system with a capacity of approximately 16 L and a total pipe length of approximately 22 m. Water was recirculated through the system by an Oberdorfer N7000S15 gear pump. The pump's max speed was 6 gpm. Flow was capped at 5 gpm due to component pressure limits. The minimum flow rate was chosen to be 0.8 gpm, under which the flow is no longer fully turbulent. With a 10 L test volume, the residence time of the system is estimated to be between 30 and 200 seconds, depending on the flow rate.

The flow loop begins with a cylindrical, steel reservoir tank with maximum capacity of 12 L and is pumped first through a 2.18 m pressure drop test section. Differential pressure was measured across the pressure drop test section by one 0-10 psi Omega PX2300 pressure transmitter. Pressure readings were recorded using an Omega DaqBoard 2000 data acquisition system. The solution then passes through a fluted tube heat exchanger with process chilled water flowing through the shell in order to maintain a steady temperature in the flow loop. The test solution then passes through the 0.91 m countercurrent cocentric tube heat exchanger. Hot water is supplied to the annulus of the heat exchanger, supplied by a 1600 W heated water bath. The solution then flows back into the reservoir tank.

Temperature measurements were done with t-type thermocouples and BAT-10 multipurpose thermometers from PhysiTemp, Inc. Temperature readings were taken

in five locations across the system: The entrance to the pressure drop section, and the entrance and exit of both the annulus and the tube of the cocentric tube heat exchanger. The latter four were used to measure temperature differences across both the tube and the annulus of the heat exchanger with an accuracy of 0.01 degC. A single helical static mixer was placed in the tube down stream of the shell and tube heat exchanger. This was to ensure a uniform temperature distribution at the outlet of the heat exchanger.

Flow rates of the test solution through the recirculating system, the chilled and the heated water in the shells of both heat exchangers were monitored using Toshiba LF-404 electromagnetic flow meters. The test solution's flow rate was controlled through the use of a motor speed controller for the recirculating pump. The chilled water flow rate was controlled using a needle valve. The flow rate of the heated water through the annulus of the cocentric tube heat exchanger was maintained at 1.9 gpm.

The differential pressure readings were used to calculate the fanning friction factor of the drag reduced flow as

$$f = \frac{\Delta P d}{2 L \rho v^2} \tag{3.1}$$

Where f is the friction factor, ΔP is the pressure drop, d is the tube diameter, L is the length over which the pressure drop was measured, v is the velocity, and ρ is the solvent density. The friction factor for water at the same flow rate was calculated using the Prandtl-Karman equation:

$$\frac{1}{\sqrt{f}} = 4 log_{10}(Re\sqrt{f}) - 0.4 \tag{3.2}$$

and Re is the solvent Reynolds number defined as

$$Re = \frac{\rho v d}{\mu} \tag{3.3}$$

where μ is the solvent dynamic viscosity. Percent drag reduction was then calculated as

$$DR = \frac{f_{solvent} - f_{DR}}{f_{solvent}} \tag{3.4}$$

Drag reduction was measured at either a fixed temperature or a fixed solvent Reynolds number. After changing system conditions, the temperatures and flow rates were allowed to reach steady state over a period of approximately one minute and held to a tolerance of ± 0.01 gpm or ± 0.1 degC.

3.3 Rheological Measurements

Shear viscosity was measured using a Anton Paar MCR500 rheometer with a CC 27, 27 mm couette geometry and a TEZ300 temperature controller. Each viscosity measurement was averaged over 5 seconds, and 50 points were measured per sweep, with each sweep ranging from 1 to 800/s. The shear rates were ramped up step wise.

3.4 Cryo-TEM

Liquid samples for cryo-TEM imaging were prepared at Ohio State University. Cryo-TEM images were taken at the Technion Laboratory for Electron Microscopy of Soft Matter, supported by the Technion Russell Berrie Nanotechnology institute (RBNI). Details of cryoTEM sample preparation have been described elsewhere, performed in the Laboratory of Electron Microscopy of Soft Matter [64, 80].

Chapter 4: Results and Discussion

4.1 Introduction and Solution Development

Because surfactant drag reducing solutions are so dilute, and attempts to degrade or otherwise change the drag reducing structures present are dampened by the relatively large mass of solvent, it is desirable to develop a switchable solution catered to specifically controlling the drag reducing nanostructures. It is also desirable that any heat transfer enhancement methods do not require any additional equipment or addition of foreign material, that would not otherwise be present in a district heat transport application. This is made more difficult by the fact that the actual structure of surfactant micelles in drag reduced flow is not fully understood. If the structure of surfactant micelles in drag reduced flow was understood, then a switch tailored to that structure could be developed from first principals. Furthermore, with better understanding, switchable solutions could be tuned on the bench scale (i.e. in a rheometer) before being tested in large scale recirculating flow loops.

In order to attempt to infer the micelle structure in drag reduced flow, literature drag reduction data was reviewed through the lens of micelle packing parameter and length trends discussed in section 2.1.4. Based on a qualitative review of the drag reduction literature, it appears that drag reducing solutions typically have a higher Reynolds number of the onset of drag reduction at higher temperatures. However,

Lu et al. incidentally showed this was not always the case [43]. In this paper, a solution of 5 mM Arquad 16-50 and 12.5 mM 4-chlorobenzoate showed the typical drag reduction curves being shifted to high flow rates with increasing temperature. This is hypothesized to be due to shortening of wormlike micelles, as discussed in section 2.1.4. However, Lu et al also showed drag reduction curves of a solution of 5 mM Arquad 16-50 and 12.5 mM 3-chlorobenzoate shifting to lower flow rates with increasing temperature, indicative of a possible structural transition occurring in the 3-chloro solution but not in the 4-chloro solution. It was hypothesized that this difference was due to differing micro structures of the quiescent state. It was predicted that typical drag reducing solutions are wormlike micelles (at least in the entire drag reducing regime), which then become progressively shorter at higher temperatures and thus the drag reduction curves shifted to progressively higher flow rates. On the other hand, it was predicted that the 3-chloro solution was initially vesicles. Using the interchangeability of shear and temperature claimed by Mendes et al, it follows that at higher temperatures it takes less shear for a vesicle to wormlike micelle transition, so the drag reduction curves get shifted to lower flow rates at increasing temperature.

These structures are tentatively confirmed by the cryo-TEM images published in Lu et al [43]; however the blotting step in taking a cryo-TEM image confounds shear effects, and a relaxation time was not specified [43]. These solutions were remade, along with various counterion ratio analogues, to probe the hypothesized structural transitions in more detail. It was anticipated that lowering the 3-chloro solution's counterion ratio to 1:1 would cause a vesicle to wormlike micelle transition, and have similar behavior to the 4-chloro solution. This was true; however, in addition, it was

discovered that 1:1 counterion ratio 3-chloro solution showed amazing and undocumented switchability. Due to constrained time, this final product was investigated and documented in more detail than the mechanistic underpinnings which this author set out to investigate.

4.2 Drag Reduction

The following scatter plot shows drag reduction vs Reynolds number and temperature of the 3-chloro switchable solution. It can be seen that DR can be sharply switched off with increasing Reynolds number, and then switched on again by a slight increase in temperature. This process can be traced reversibly along a 3D path on a scatterplot of DR vs temperature vs Reynolds number. The data shown is a composition of three different batches of the 3-chloro solution. This data was taken by several different experimenters on solutions of various ages. There is also some messiness in this data due to a hysteresis that sometimes occurs in both the temperature and Reynolds number shift. The amount of hystersis varies by how quickly the experiment is ran. The temperature-shear superposition can be seen more clearly in a subset from a single experiment taken by one experimenter in one day on one batch of the solution in figure 4.2. This flow rate "switch" occurs over less than 0.01 gpm(the resolution of the flow meter used) in half inch tubing. To get the apparently vertical data in the following graphs, the temperature and/or flow rate was allowed to slowly increase or slowly decrease over several minutes, effectively interpolating between flow rate or temperature measurements.

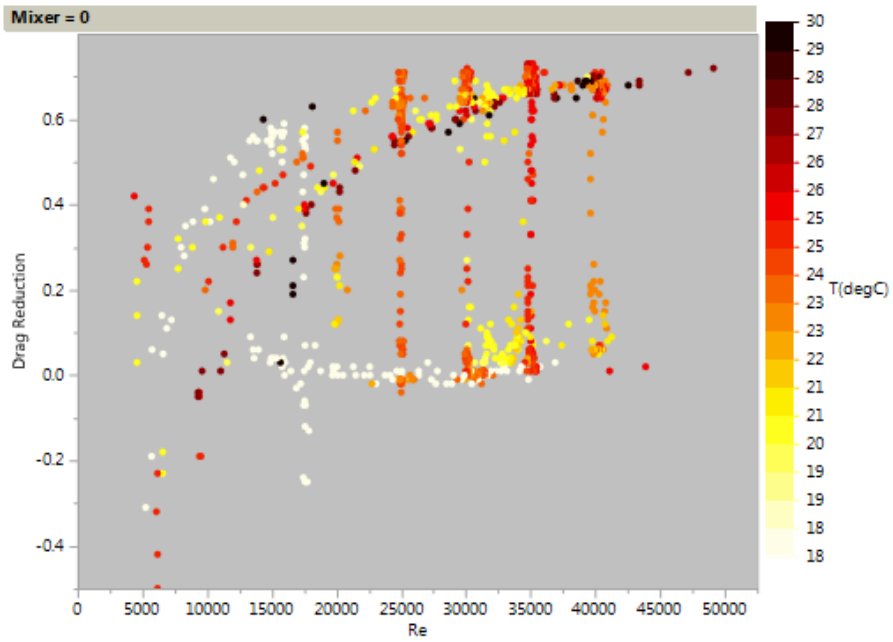

Figure 4.1: Drag reduction vs Reynolds number at various temperatures of 5mM Arquad 16-50, 5 mM 3-chloro benzoic acid, 5 mM NaOH

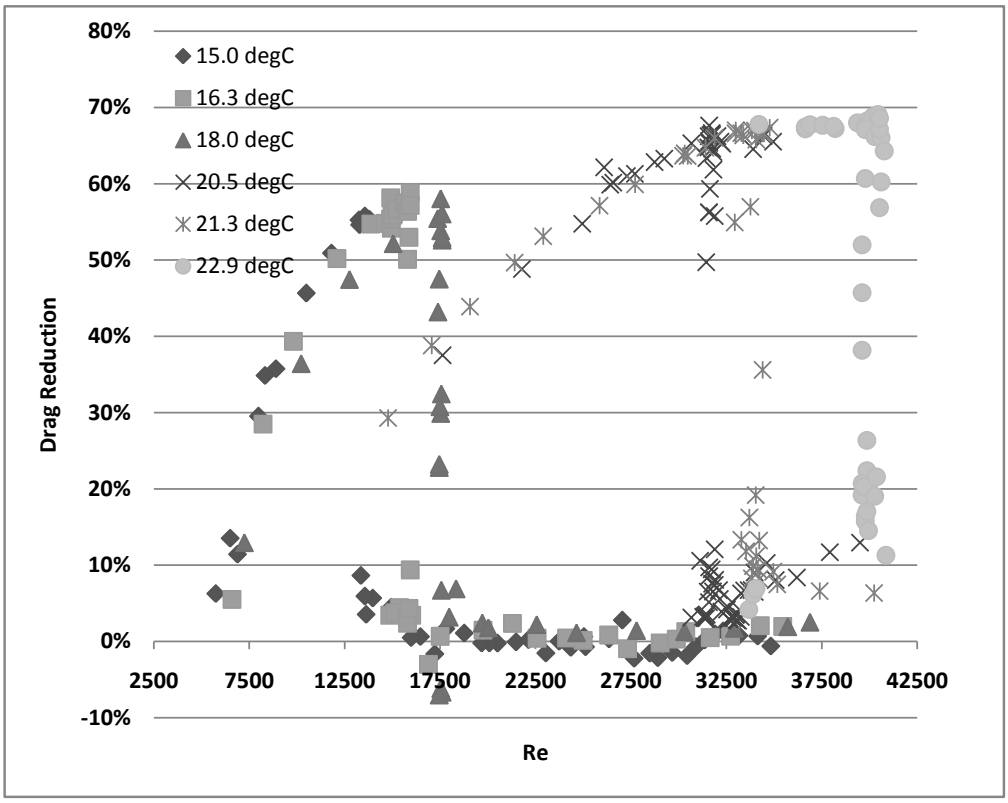

Figure 4.2: Subset of drag reduction vs Reynolds number data at various temperatures of 5mM Arquad 16-50, 5 mM 3-chloro benzoic acid, 5 mM NaOH

More precisely documented experimentation would be required to separate the cause of variation between solution batches and experiments.

Figure 4.3 is a subset of the data showing the temperature "switch". The switch can occur over as little as 0.1 degrees Celsius. This data subset also illustrates the importance of hystersis in this system.

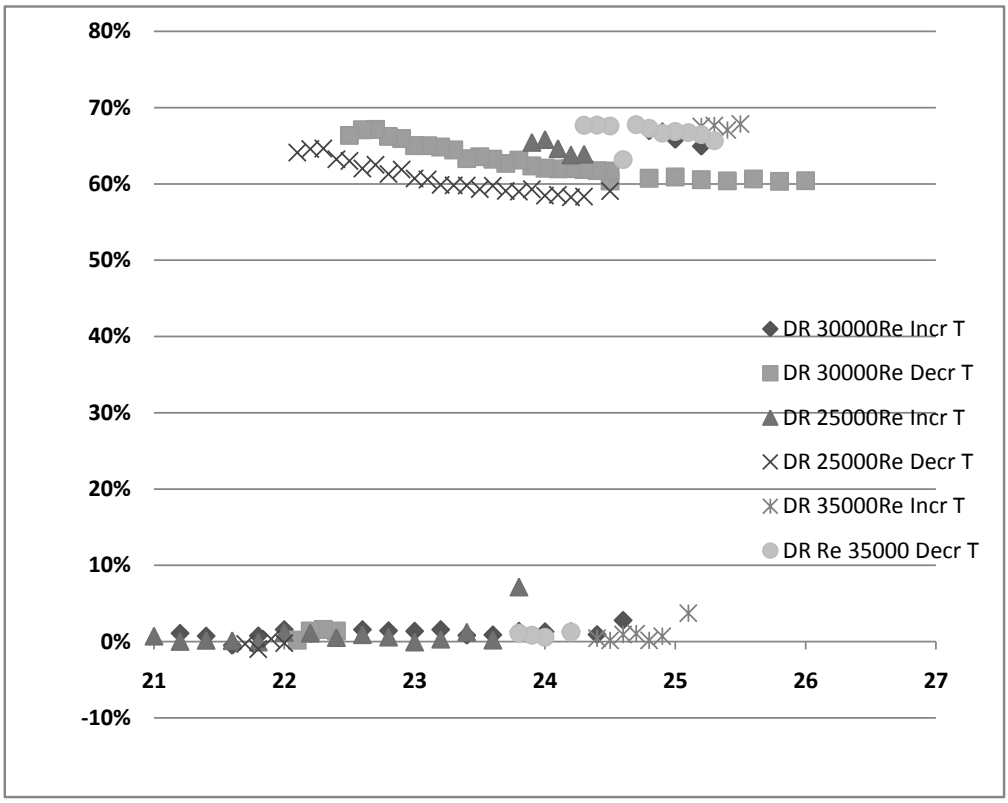

Figure 4.3: Drag reduction vs temperature at various Reynolds Numbers of 5mM Arquad 16-50, 5 mM 3-chloro benzoic acid, 5 mM NaOH

Both the flow rate and temperature "switch" occurred in seconds.

4.3 Rheology

The following two sets of graphs show shear viscosity vs shear rate for 3 different counterion ratios of the 3-chlorobenzoate and 5 mM Arquad 16-50. Also shown for reference is 2.5 to 1 4-chlorobenzoate 5 mM Arquad 16-50, and completely typical surfactant drag reducing solution. The first set of graph groups the data by temperature while the second set groups the data by counterion ratio.

It can be seen that the switchable (3-chloro) solutions show an unusual dip in the shear viscosity at intermediate shear rates. This dip, at low temperatures tends to flatten and converge to the typical drag reducing solution at higher counterion ratios. At higher temperatures, the dip is unaffected by increasing the counterion ratio.

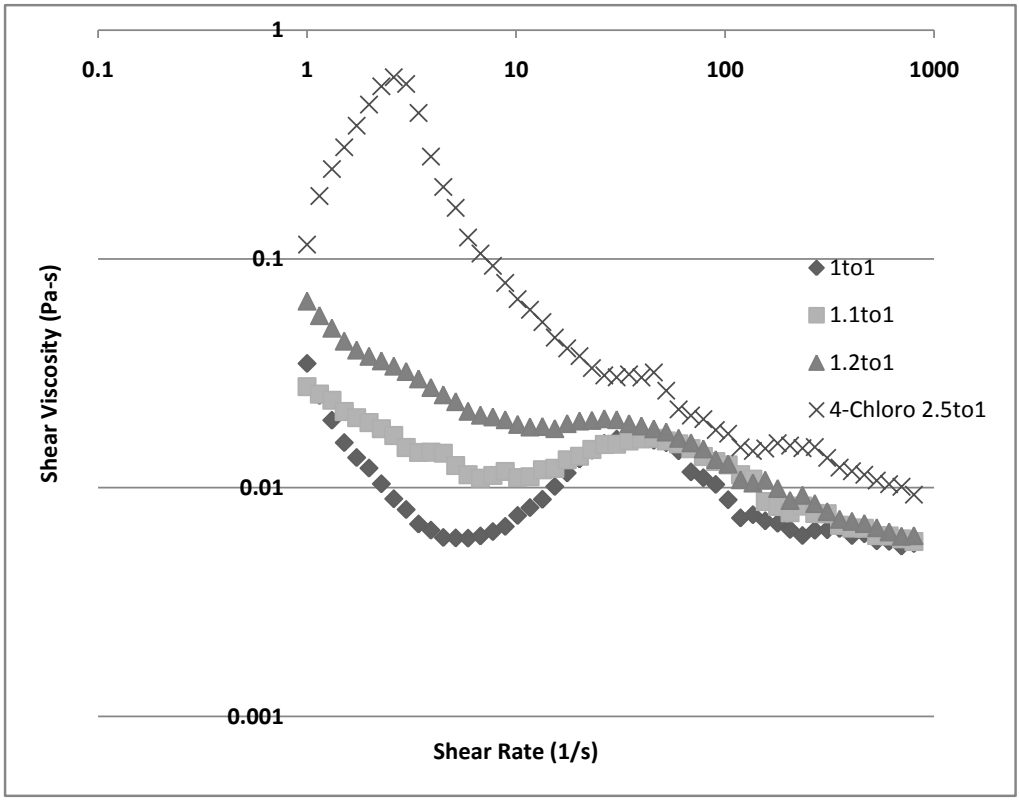

Figure 4.4: Shear viscosity vs shear rate of 5 mM Arquad 16-50 with 5, 5.5, or 6 mM 3-chloro benzoic acid (with 5, 5.5, or 6mM NaOH respectively) or 12.5 mM 4-chloro benzoic acid and 12.5 mM NaOH at 20 degrees Celsius.

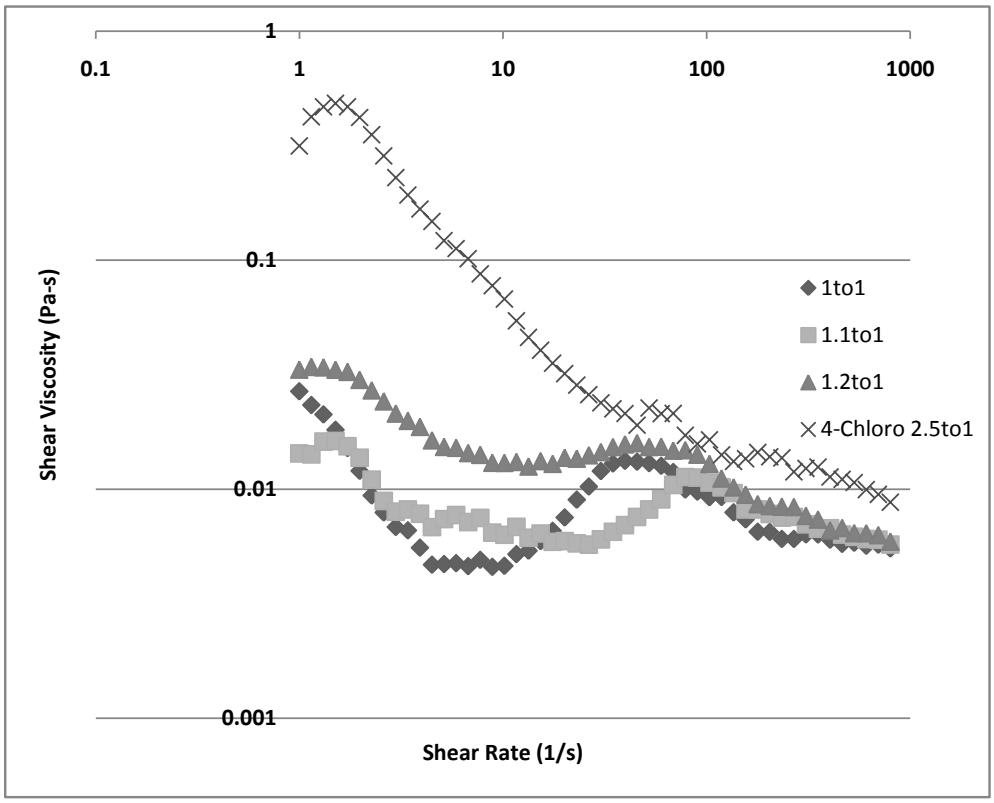

Figure 4.5: Shear viscosity vs shear rate of 5 mM Arquad 16-50 with 5, 5.5, or 6 mM 3-chloro benzoic acid (with 5, 5.5, or 6mM NaOH respectively) or 12.5 mM 4-chloro benzoic acid and 12.5 mM NaOH at 22.5 degrees Celsius.

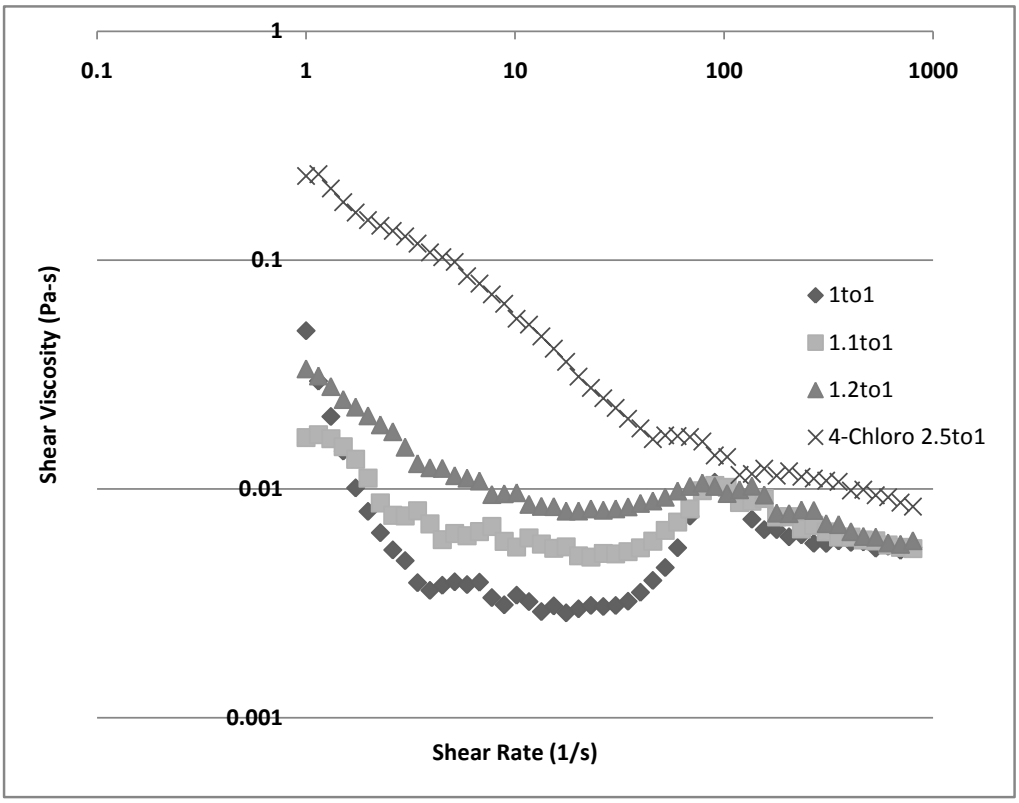

Figure 4.6: Shear viscosity vs shear rate of 5 mM Arquad 16-50 with 5, 5.5, or 6 mM 3-chloro benzoic acid (with 5, 5.5, or 6mM NaOH respectively) or 12.5 mM 4-chloro benzoic acid and 12.5 mM NaOH at 25 degrees Celsius.

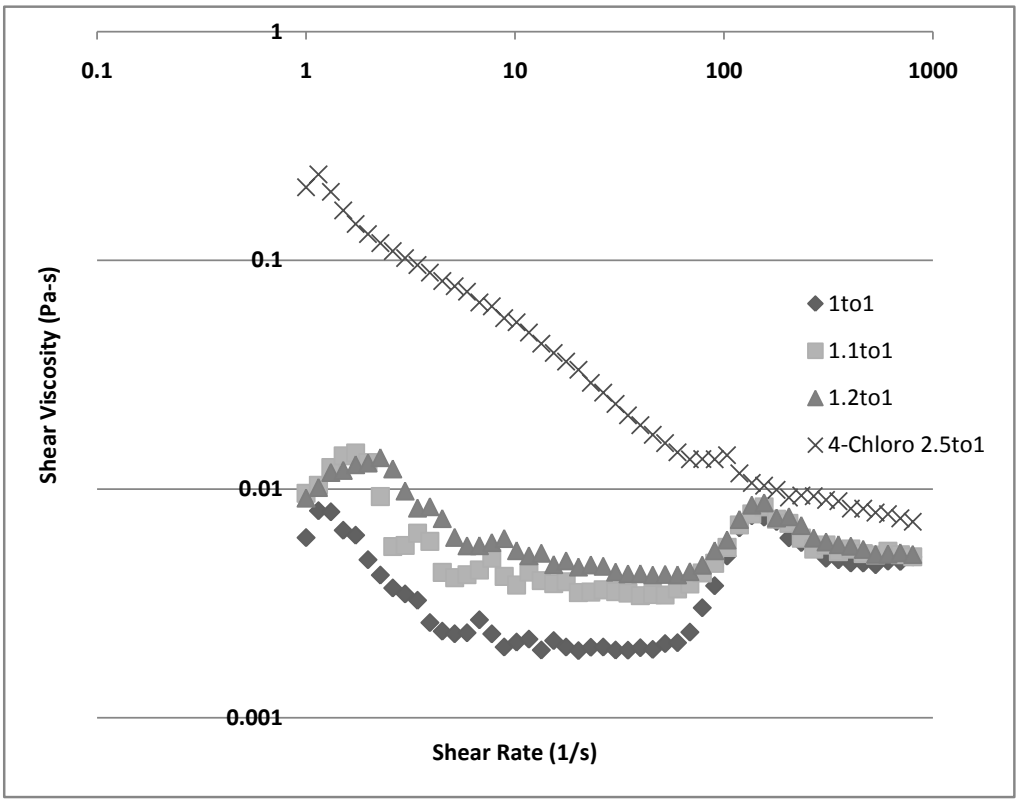

Figure 4.7: Shear viscosity vs shear rate of 5 mM Arquad 16-50 with 5, 5.5, or 6 mM 3-chloro benzoic acid (with 5, 5.5, or 6mM NaOH respectively) or 12.5 mM 4-chloro benzoic acid and 12.5 mM NaOH at 30 degrees Celsius.

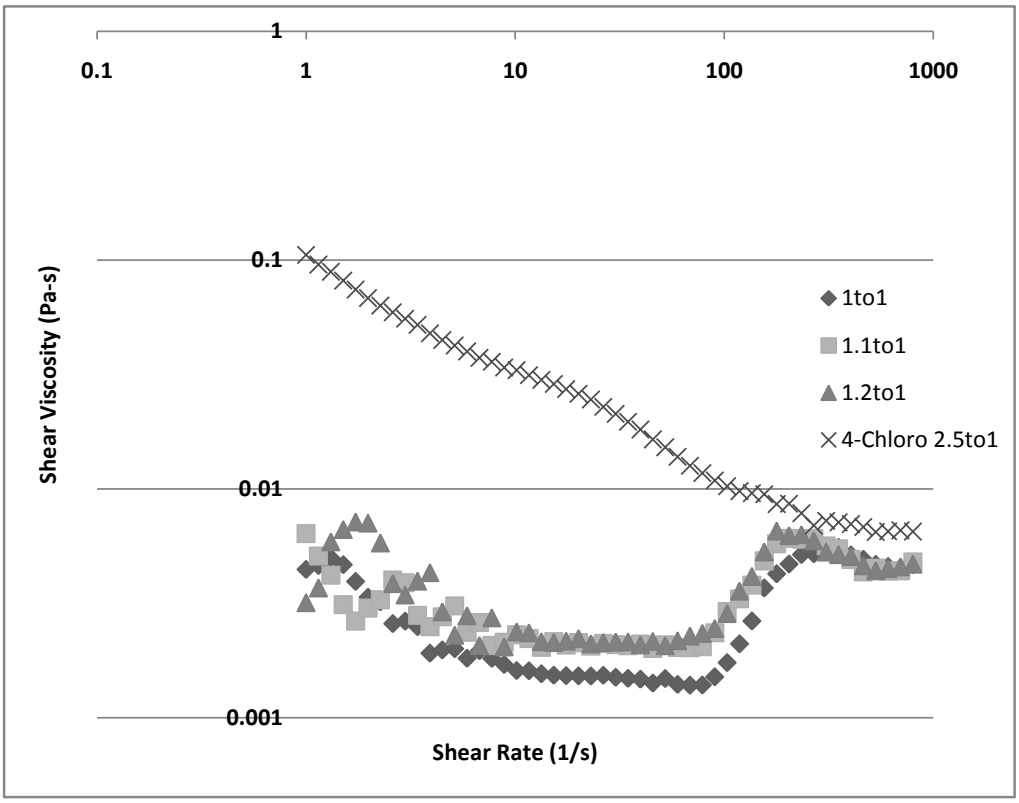

Figure 4.8: Shear viscosity vs shear rate of 5 mM Arquad 16-50 with 5, 5.5, or 6 mM 3-chloro benzoic acid (with 5, 5.5, or 6mM NaOH respectively) or 12.5 mM 4-chloro benzoic acid and 12.5 mM NaOH at 35 degrees Celsius.

Also, the end of the dip is shifted to progressively higher shear rates at progressively higher temperatures. This shifting matches the shifts seen in the drag reducing data - if the end of the dip corresponds to where the drop off in drag reduction occurs, then the increasing shear rate before the dip ends with increase temperature corresponds to the increase in Re of the drop off of drag reducing data with increasing temperature.

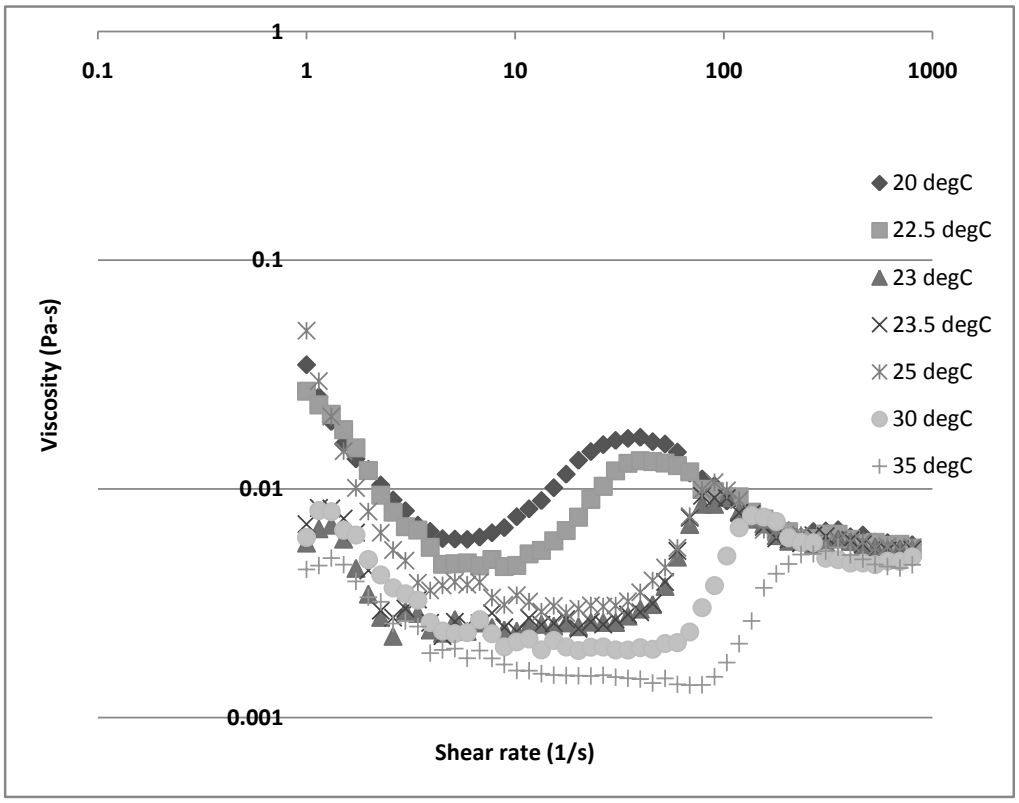

Figure 4.9: Shear viscosity vs shear rate of 5 mM Arquad 16-50, 5 mM 3-chloro benzoic acid, 5 mM NaOH at various temperatures

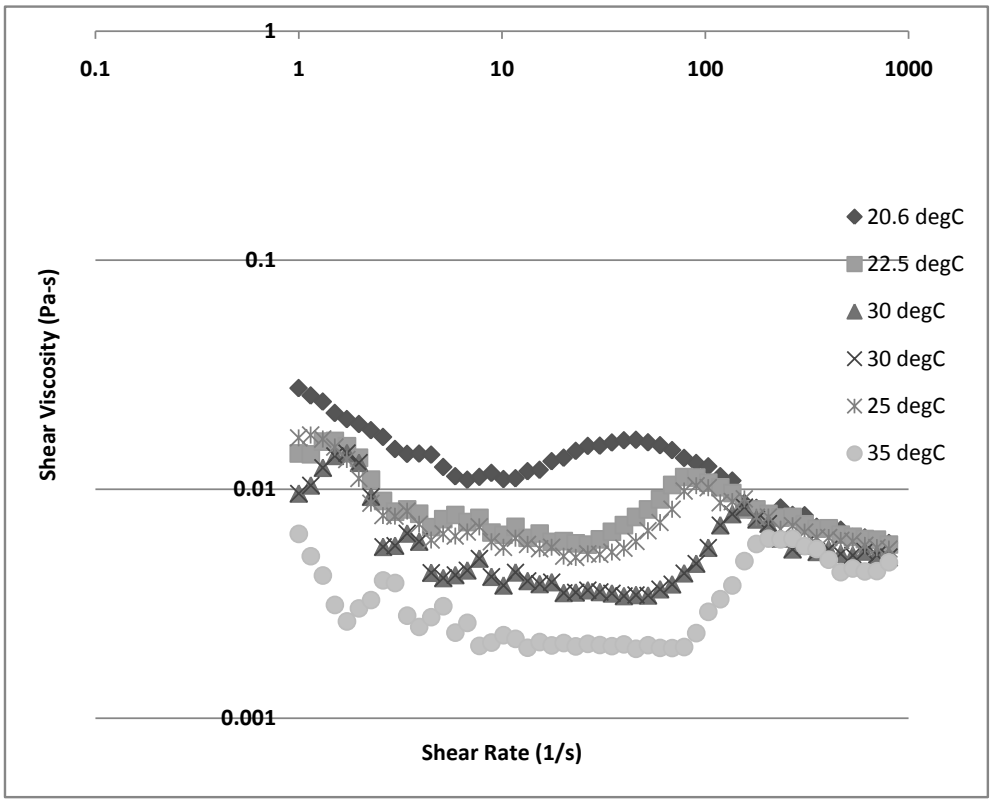

Figure 4.10: Shear viscosity vs shear rate of 5 mM Arquad 16-50, 5.5 mM 3-chloro benzoic acid, 5.5 mM NaOH at various temperatures

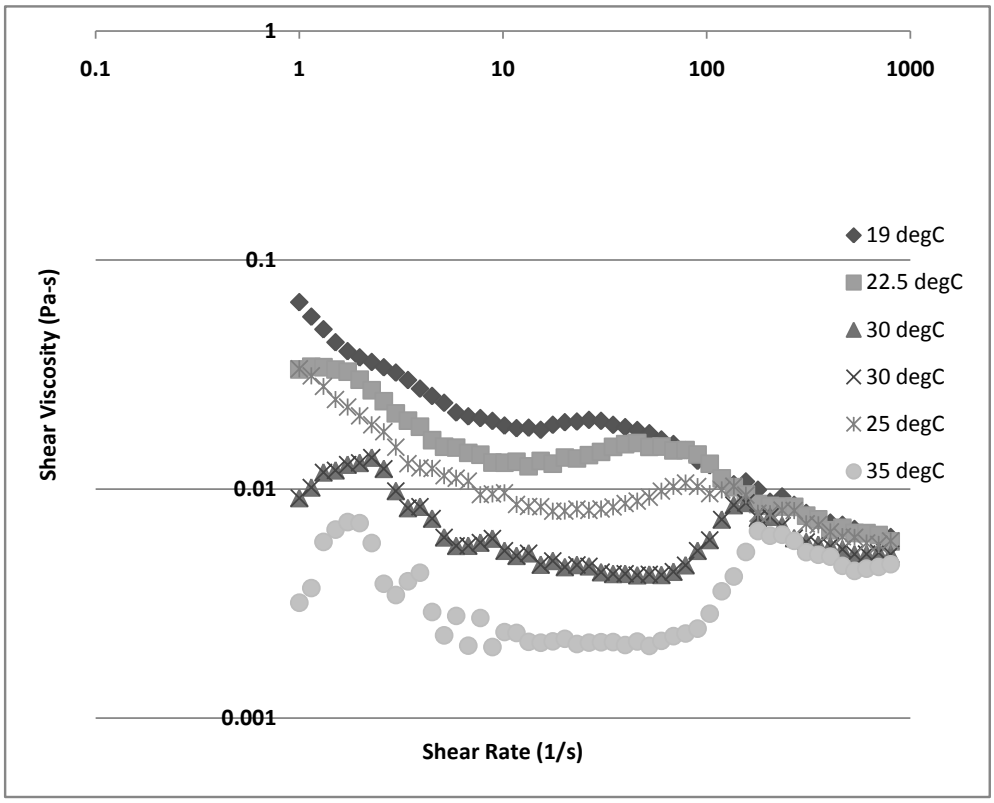

Figure 4.11: Shear viscosity vs shear rate of 5 mM Arquad 16-50, 6 mM 3-chloro benzoic acid, 6 mM NaOH at various temperatures

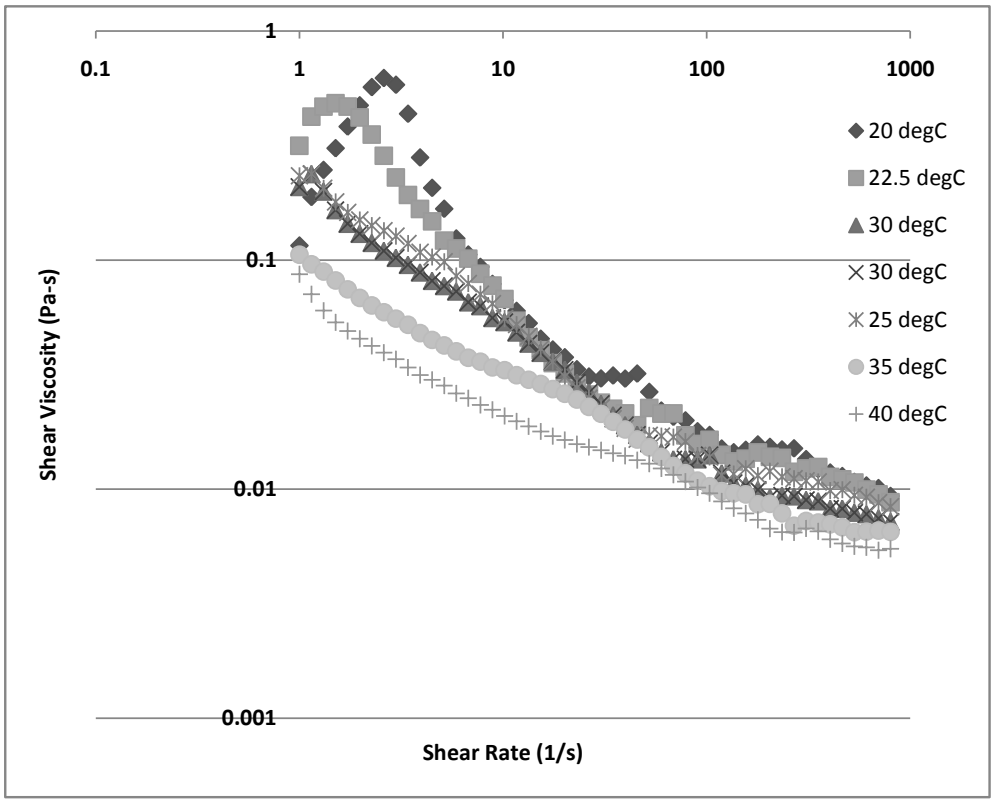

Figure 4.12: Shear viscosity vs shear rate of 5 mM Arquad 16-50, 12.5 mM 4-chloro benzoic acid, 12.5 mM NaOH at various temperatures

As far as this author knows, this is the only so direct correlation between drag reduction and rheology data.

The slope of the growth of the hump in the shear viscosity vs shear rate curves was plotted vs temperature, at the suggestion of Dr. Robert Brodkey. Although more data is required, it appears to have some Arrhenius-like behavior, which can be likened to some of Dr. Brodkey's early work in his kinetic theory of polymer rheology [5].

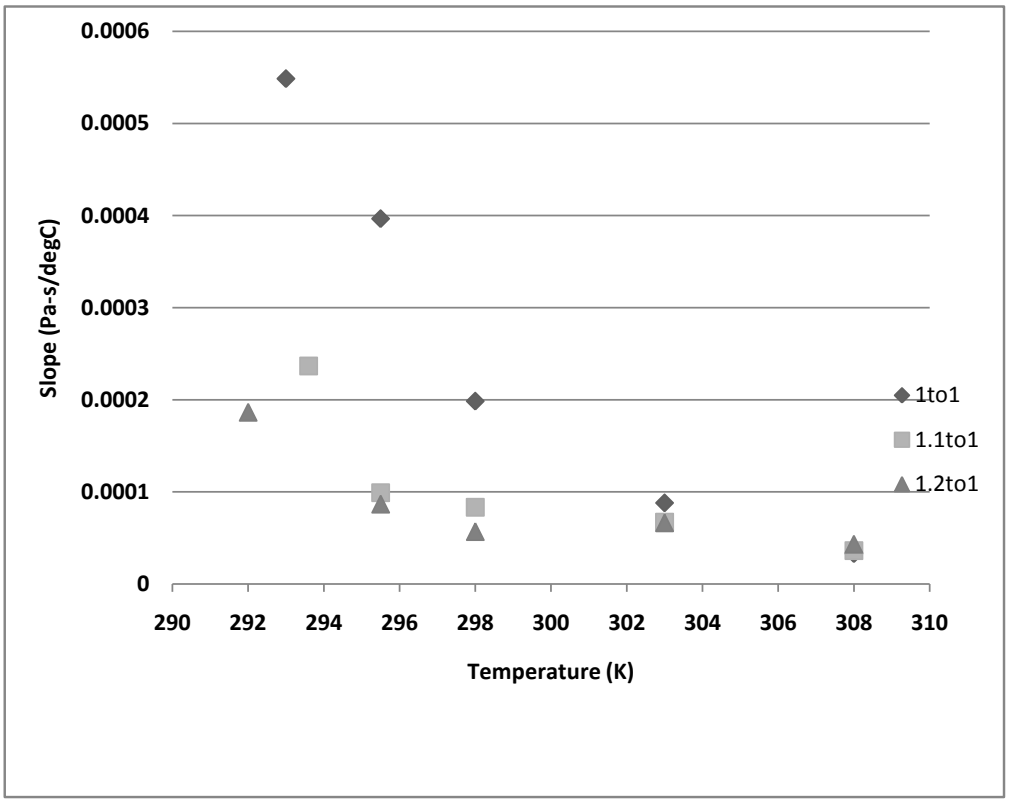

Figure 4.13: Slope of growth of shear viscosity hump vs temperature at 1to1, 1.1to1, and 1.2to1 counterion to surfactant ratios of the 5 mM Arquad 16-50, X mM 3-chloro benzoic acid, and X mM NaOH

A similar shear viscosity curve can be seen in the following figure of 5 mM Arquad 16-50 with 5 mM dimethyl benzoate from Qi et al.

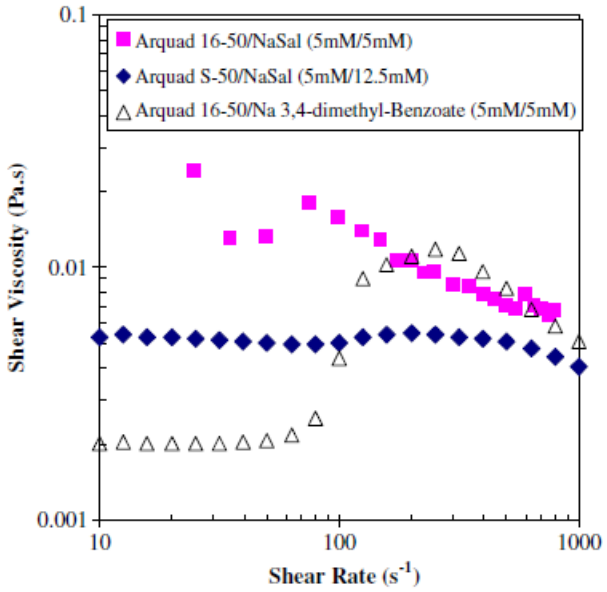

Figure 4.14: Shear viscosity vs shear rate from [59]

Both the dimethyl and the chloro benzoate substitutents are highly hydrophobic.

4.4 Cryo-TEM

Cryo-TEM images were taken at 18 degrees Celsius and 30 degrees Celsius. At each temperature, images were taken with and without a relaxation time before vitrifying the specimen. These conditions were intended to show the structure above and below the shear "switch" loss of drag reduction - the 18 degrees Celsius sample would shear switch while the 30 degrees Celsius sample would not.

The 30 degrees Celsius images show unusual membrane like agglomerates of threadlike micelles. The constituent threadlike micelles are very visible in figure 4.16, taken after a 10 second relaxation before vitrification. Prof. Talmon, a world expert in

imaging of surfactant micelles, has never seen structures like these sheets of aggregated threadlike micelles. The image taken without a relaxation is a nearly uniform membrane.

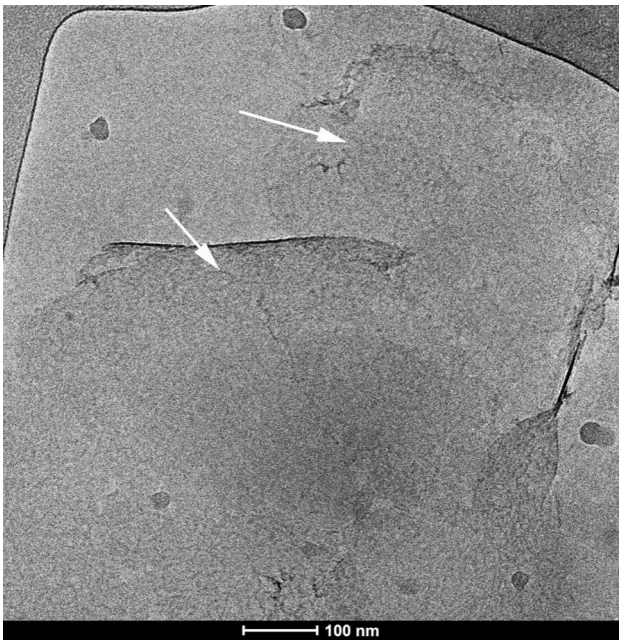

Figure 4.15: Cryo-TEM image of 5 mM Arquad 16-50, 5 mM 3-chloro benzoic acid, 5 mM NaOH vitrified from 30 degrees Celsius with no relaxation time

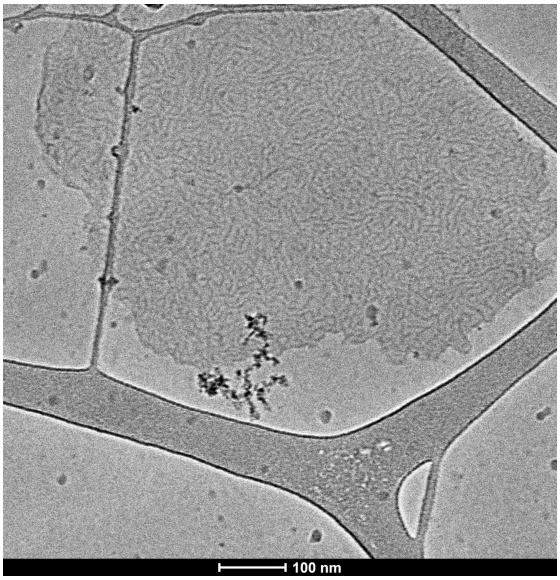

Figure 4.16: Cryo-TEM image of 5 mM Arquad 16-50, 5 mM 3-chloro benzoic acid, 5 mM NaOH vitrified from 30 degrees Celsius with 10 seconds relaxation time

At 18 degrees Celsius, very long and unbranched wormlike micelles were present. The image taken without relaxation showed near perfectly aligned micelles, while the sample with a 30 second relaxation was entangled and randomly oriented.

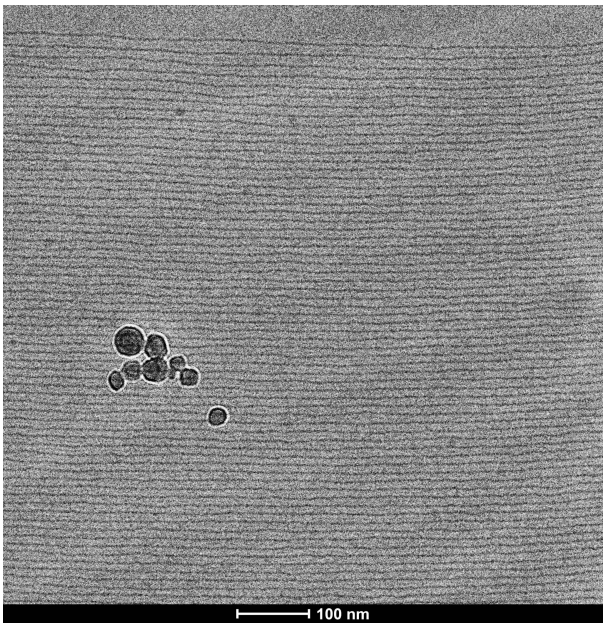

Figure 4.17: Cryo-TEM image of 5 mM Arquad 16-50, 5 mM 3-chloro benzoic acid, 5 mM NaOH vitrified from 18 degrees Celsius with no relaxation time

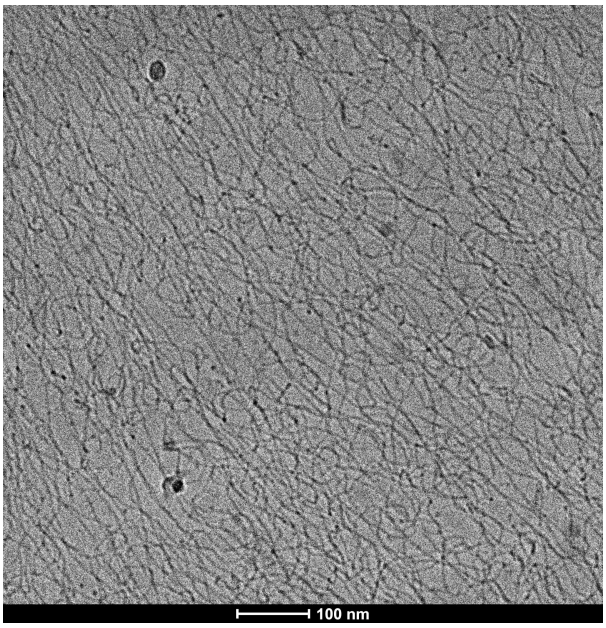

Figure 4.18: Cryo-TEM image of 5 mM Arquad 16-50, 5 mM 3-chloro benzoic acid, 5 mM NaOH vitrified from 18 degrees Celsius with 30 seconds relaxation time

These increase in packing parameter with increasing temperature shown in the Cryo-TEM images does not match prior work, discussed in sections 2.3.3 and 2.1.4. Furthermore, no dramatic structural transition occurred between with and without a relaxation at 18 degrees Celsius. In fact, a dramatic structural transition was present with and without relaxation of the 30 degrees Celsius images.

4.5 Solution Tunability

The temperature/shear rate switch can be tuned with a constant composition. The average shear rate in the tube, calculated as

$$\gamma = \frac{8v}{D} \tag{4.1}$$

where v is the bulk velocity and D is the diameter of the tube, was plotted vs the temperature at the sudden loss of drag reduction. The drag reduction data used is the subset shown in figure 4.2. Also, the shear rate at the onset of the hump in the viscosity curve was plotted vs temperatures. Both of these show a qualitatively linear correlation. Of course, there is a broad distribution of shear rates in tube flow (and a narrow distribution in couette flow). A better choice of tube shear rate and a broader experimental range may tie these correlations together more strongly.

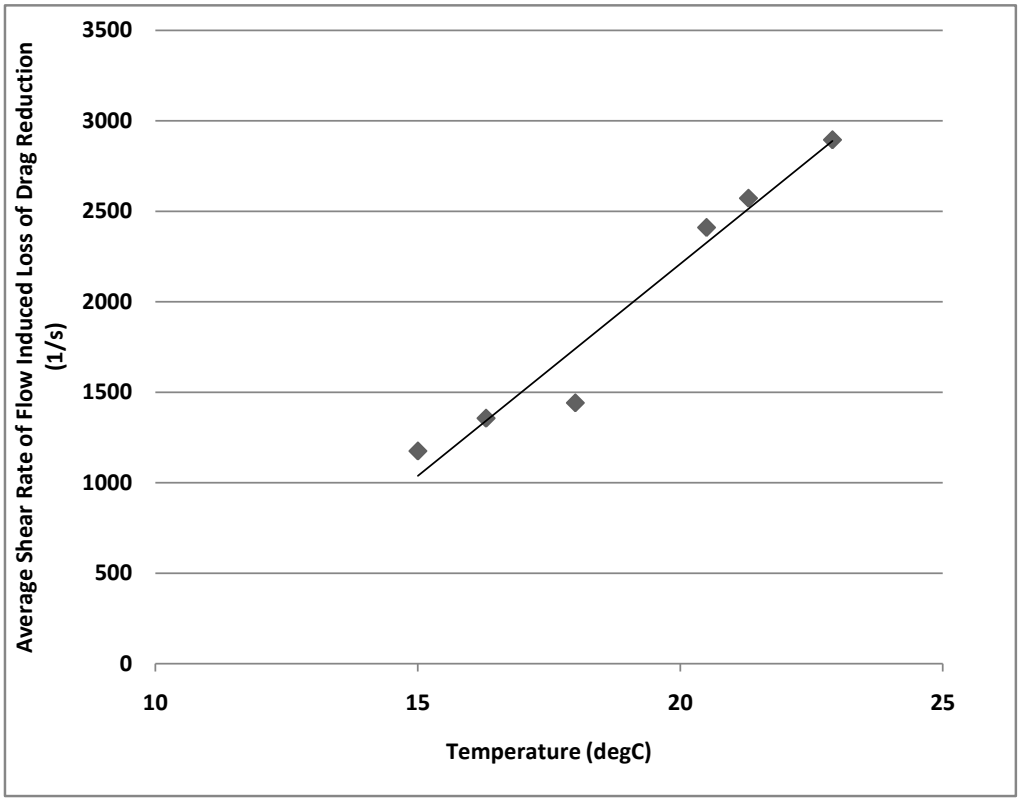

Figure 4.19: 5 mM Arquad 16-50, 5 mM 3-chloro benzoic acid, 5 mM NaOH sudden loss of drag reduction vs temperature

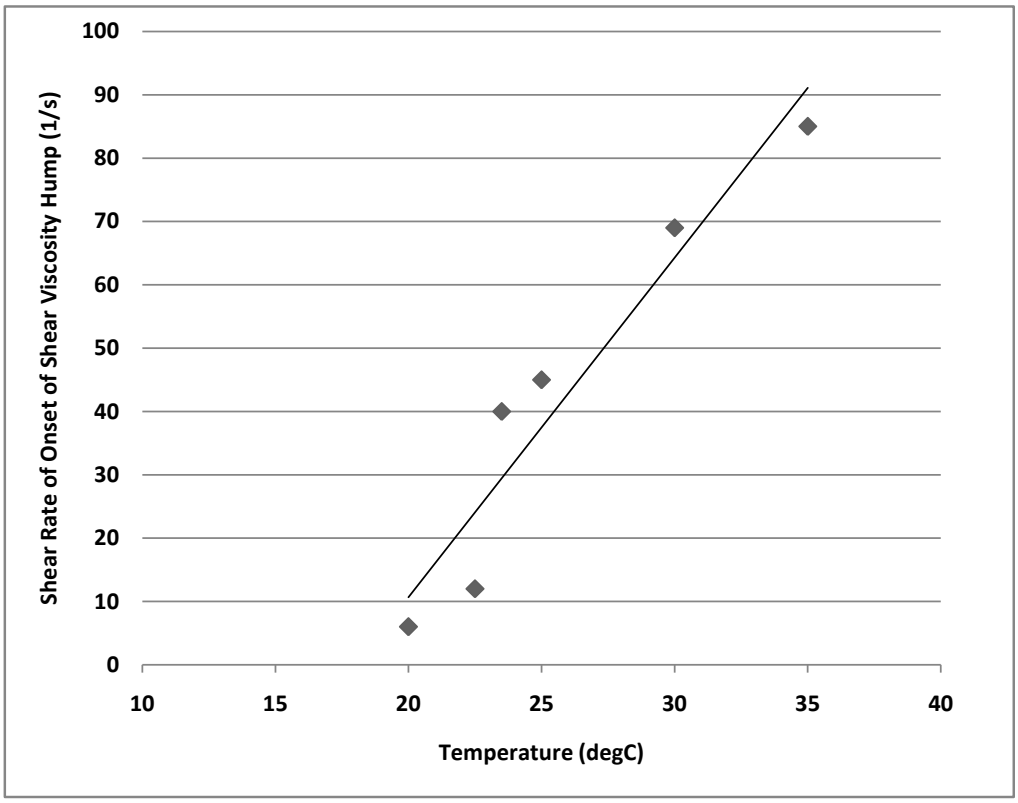

Figure 4.20: 5 mM Arquad 16-50, 5 mM 3-chloro benzoic acid, 5 mM NaOH onset of shear viscosity hump vs temperature.

Chapter 5: Conclusions

1. A switchable, "smart" drag reducing solution was developed.

2. The switchable "3-chloro" solution shows a 70% change in drag reduction with only a 0.01 gpm change of flow rate(hundreds of Re).

3. The switchable "3-chloro" solution shows a 70% change in drag reduction with only a 0.1 degC change in temperature.

4. The switch happens in a matter of seconds.

5. A hump in the shear viscosity data correlates with the drop in drag reduction data.

6. It is believed that with a better choice of tube shear rate, rheology data can, for the first time, be used to predict surfactant drag reduction results.

7. It is believed that the "3-chloro" solution can be tuned by changing surfactant molecular parameters (eg tail length) and counterion ratio to shift the "switch" based on an individual system's requirements.

8. It is believed that after developing drag reduction-rheology correlations and exploring the effect of molecular parameters on shifts in the drag reduction curves,

a customer could approach us with a set of flow rate, tube diameter, temperature, etc. conditions and this solution could be tuned to have optimal heat transfer and drag reduction, and that this tuning can be done in a rheometer (using a few mL samples) instead of in a drag reduction test loop (few L to 10 of L samples).

Bibliography

[1] Guillermo Aguilar, Kazimir Gasljevic, and Eric F. Matthys. Asymptotes of maximum friction and heat transfer reductions for drag-reducing surfactant solutions. *International Journal of Heat and Mass Transfer*, 44(15):2835–2843, 2001.

[2] Bellamy. Recovery of surfactant-based friction reduction downstream of shearing obstructions,. In *2001 FRA Meeting*.

[3] H. W. Bewersdorff and D. Ohlendorf. The behaviour of drag-reducing cationic surfactant solutions. *Colloid & Polymer Sci*, 266(10):941–953, 1988.

[4] Hans-Werner Bewersdorff. Drag reduction in surfactant solutions. In *Structure of Turbulence and Drag Reduction*, pages 293–312. Springer Berlin Heidelberg, 1990.

[5] Robert Brodkey. Private correspondence on march 12, 2018. .

[6] E.D. Burger, W.R. Munk, and H.A. Wahl. Flow increase in the trans alaska pipeline through use of a polymeric drag-reducing additive. *Journal of Petroleum Technology*, 34(02):377–386, 1982.

[7] Paul D. Butler, L.J. Magid, William A. Hamilton, P.J. Kreke, and John B. Hayter. Effects of shear on the structures in a system of small rodlike micelles. In *Mat. Res. Soc. Symp. Proc.*

[8] Yujun Feng Cecile Dreiss. *Wormlike Micelles: Advances in Systems, Characterisation and Applications (Soft Matter Series)*. Royal Society of Chemistry, 2017.

[9] Zdenek Chara, Jacques L. Zakin, Miroslav Severa, and Jiri Myska. Turbulence measurements of drag reducing surfactant systems. *Experiments in Fluids*, 16(1):36–41, nov 1993.

[10] R. N. Christensen and J. L. Zakin. Drag and heat transfer reduction in circular tubes and plate fin heat exchangers. *Proceedings International District Heating and Cooling Assoc*, 81:189–202, 1991.

[11] T. M. Clausen, P. K. Vinson, J. R. Minter, H. T. Davis, Y. Talmon, and W. G. Miller. Viscoelastic micellar solutions: microscopy and rheology. *The Journal of Physical Chemistry*, 96(1):474–484, jan 1992.

[12] J.H. Clint. *Surfactant Aggregation*. Springer, 2012.

[13] Vania Croce, Terence Cosgrove, Geoff Maitland, Trevor Hughes, and Göran Karlsson. Rheology, cryogenic transmission electron spectroscopy, and small-angle neutron scattering of highly viscoelastic wormlike micellar solutions. *Langmuir*, 19(20):8536–8541, sep 2003.

[14] P.V. Danckwerts. Continuous flow systems. *Chemical Engineering Science*, 2(1):1–13, feb 1953.

[15] Pierre-Gilles de Gennes. *Introduction to Polymer Dynamics (Lezioni Lincee)*. Cambridge University Press, 1990.

[16] J Drappier, T Divoux, Y Amarouchene, F Bertrand, S Rodts, O Cadot, J Meunier, and Daniel Bonn. Turbulent drag reduction by surfactants. *Europhysics Letters (EPL)*, 74(2):362–368, apr 2006.

[17] A. G. Fabula. Fire-fighting benefits of polymer friction reduction. *Journal of Basic Engineering*, 1971.

[18] F. Forrest and G.A.H. Grierson. Friction losses in cast iron pipe carrying paper stock. *Paper Trade Journal*, 92(22):39–41, 1931.

[19] Y.F. Fu, C.Q. Yuan, and X.Q. Bai. Marine drag reduction of shark skin inspired riblet surfaces. *Biosurface and Biotribology*, 3(1):11–24, mar 2017.

[20] Koji Fukagata, Kaoru Iwamoto, and Nobuhide Kasagi. Contribution of reynolds stress distribution to the skin friction in wall-bounded flows. *Physics of Fluids*, 14(11):L73–L76, nov 2002.

[21] H. W. Bewersdorff G. Dembek. Short time increase sewer capacity by addition of water soluble polymers. *GWF WasserAbwasser*, 1981.

[22] K. Gasljevic. *An experimental investigation of drag reduction by surfactant solutions and of its implementation in hydronic systems*. PhD thesis, University of California Santa Barbara, 1995.

[23] Ruisheng Guo and Feng Zhou. Superhydrophobic surfaces for drag reduction. In *Encyclopedia of Tribology*, pages 3380–3387. Springer US, 2013.

[24] W.A. Hamilton, P.D. Butler, John B. Hayter, L.J. Magid, and P.J. Kreke. "over the horizon" SANS: Measurements on near-surface poiseuille shear-induced ordering of dilute solutions of threadlike micelles. *Physica B: Condensed Matter*, 221(1-4):309–319, apr 1996.

[25] P. A. Hassan, S. J. Candau, F. Kern, and C. Manohar. Rheology of wormlike micelles with varying hydrophobicity of the counterion. *Langmuir*, 14(21):6025–6029, oct 1998.

[26] P. A. Hassan, B. S. Valaulikar, C. Manohar, F. Kern, L. Bourdieu, and S. J. Candau. Vesicle to micelle transition: rheological investigations. *Langmuir*, 12(18):4350–4357, jan 1996.

[27] Paul C. Hiemenz and Raj Rajagopalan. *Principles of Colloid and Surface Chemistry, Third Edition, Revised and Expanded (UNDERGRADUATE CHEMISTRY SERIES)*. CRC Press, 1997.

[28] Yuntao Hu and Eric F. Matthys. Characterization of micellar structure dynamics for a drag-reducing surfactant solution under shear: normal stress studies and flow geometry effects. *Rheologica Acta*, 34(5):450–460, 1995.

[29] Yasuo Kawaguchi, Takehiko Segawa, Ziping Feng, and Peiwen Li. Experimental study on drag-reducing channel flow with surfactant additives—spatial structure of turbulence investigated by PIV system. *International Journal of Heat and Fluid Flow*, 23(5):700–709, 2002.

[30] S. L. Keller, P. Boltenhagen, D. J. Pine, and J. A. Zasadzinski. Direct observation of shear-induced structures in wormlike micellar solutions by freeze-fracture electron microscopy. *Physical Review Letters*, 80(12):2725–2728, mar 1998.

[31] C.A Kim, J.T Kim, K Lee, H.J Choi, and M.S Jhon. Mechanical degradation of dilute polymer solutions under turbulent flow. *Polymer*, 41(21):7611–7615, 2000.

[32] Akira Kishimoto, Hiroshi Usui, and Hiroshi Suzuki. Influences of the inner-surface conditions of circular tubes on the heat transfer in a surfactant drag-reduction system. *Kagaku Kogaku Ronbunshu*, 27(3):347–366, 2001.

[33] Palle Laugesen, Jan Elleriis, Thomas Østergaard, Jens Busk, and Flemming Hammer. *Anvendelse Af Glat Vand: Konsekvenser for Økonomi*. Energiministeriets Forskningsudvalg for Produktion og Fordeling af El og Varme, Denmark, 2000.

[34] F Lequeux. Reptation of connected wormlike micelles. *Europhysics Letters (EPL)*, 19(8):675–681, aug 1992.

[35] F.-C. Li, Y. Kawaguchi, K. Hishida, and M. Oshima. Investigation of turbulence structures in a drag-reduced turbulent channel flow with surfactant additive by stereoscopic particle image velocimetry. *Experiments in Fluids*, 40(2):218–230, oct 2005.

[36] Feng-Chen Li, Yasuo Kawaguchi, Bo Yu, Jin-Jia Wei, and Koichi Hishida. Experimental study of drag-reduction mechanism for a dilute surfactant solution flow. *International Journal of Heat and Mass Transfer*, 51(3-4):835–843, 2008.

[37] Feng-Chen Li, Bo Yu, Jin-Jia Wei, and Yasuo Kawaguchi. *Turbulent Drag Reduction by Surfactant Additives*. Wiley, 2012.

[38] Yiyang Lin, Xue Han, Jianbin Huang, Honglan Fu, and Cailan Yu. A facile route to design pH-responsive viscoelastic wormlike micelles: Smart use of hydrotropes. *Journal of Colloid and Interface Science*, 330(2):449–455, 2009.

[39] Z. Lin. Branched worm-like micelles and their networks. *Langmuir*, 12(7):1729–1737, jan 1996.

[40] Z Lin, Y Zheng, H.T Davis, L.E Scriven, Y Talmon, and J.L Zakin. Unusual effects of counterion to surfactant concentration ratio on viscoelasticity of a cationic surfactant drag reducer. *Journal of Non-Newtonian Fluid Mechanics*, 93(2-3):363–373, oct 2000.

[41] Zhiqing Lin, Bin Lu, Jacques L. Zakin, Yeshayahu Talmon, Yi Zheng, H.Ted Davis, and L.E. Scriven. Influence of surfactant concentration and counterion to surfactant ratio on rheology of wormlike micelles. *Journal of Colloid and Interface Science*, 239(2):543–554, 2001.

[42] Zhiqing Lin, Anthony Mateo, Yi Zheng, Ellina Kesselman, Eric Pancallo, David Hart, Yeshayahu Talmon, Ted Davis, Scriven L., and Jacques Zakin. Comparison of drag reduction, rheology, microstructure and stress-induced precipitation of dilute cationic surfactant solutions with odd and even alkyl chains. *Rheologica Acta*, 41(6):483–492, jan 2002.

[43] B. Lu, X. Li, L. E. Scriven, H. T. Davis, Y. Talmon, and J. L. Zakin. Effect of chemical structure on viscoelasticity and extensional viscosity of drag-reducing cationic surfactant solutions. *Langmuir*, 14(1):8–16, 1998.

[44] B. Lu, Y. Zheng, H. T. Davis, L. E. Scriven, Y. Talmon, and J. L. Zakin. Effect of variations in counterion to surfactant ratio on rheology and microstructures of drag reducing cationic surfactant systems. *Rheologica Acta*, 37(6):528–548, 1998.

[45] Fankhanel M., Icking M., Althaus W., Steiff A., and Weinspach M. Application of drag reducing additives in district heating systems. *District heating international*, 19(2), 1990.

[46] L. J. Magid, Z. Han, Z. Li, and P. D. Butler. Tuning the contour lengths and persistence lengths of cationic micelles the role of electrostatics and specific ion binding. *The Journal of Physical Chemistry B*, 104(29):6717–6727, jul 2000.

[47] Angelos Malliaris, Jacques Le Moigne, Jean Sturm, and Raoul Zana. Temperature dependence of the micelle aggregation number and rate of intramicellar excimer formation in aqueous surfactant solutions. *The Journal of Physical Chemistry*, 89(12):2709–2713, jun 1985.

[48] Andrew Maxson, Lucas Watson, Prathamesh Karandikar, and Jacques Zakin. Heat transfer enhancement in turbulent drag reducing surfactant solutions by agitated heat exchangers. *International Journal of Heat and Mass Transfer*, 109:1044–1051, jun 2017.

[49] Sylvio May, Yardena Bohbot, and Avinoam Ben-Shaul. Molecular theory of bending elasticity and branching of cylindrical micelles. *The Journal of Physical Chemistry B*, 101(43):8648–8657, oct 1997.

[50] E. Mendes, Janaky Narayanan, R. Oda, F. Kern, S. J. Candau, and C. Manohar. Shear-induced vesicle to wormlike micelle transition. *The Journal of Physical Chemistry B*, 101(13):2256–2258, mar 1997.

[51] H. Mizunuma, T. Kobayashi, and S. Tominaga. Drag reduction and heat transfer in surfactant solutions with excess counterion. *Journal of Non-Newtonian Fluid Mechanics*, 165(5-6):292–298, 2010.

[52] Y. Moroi. *Micelles: Theoretical and Applied Aspects (The Language of Science)*. Springer, 1992.

[53] K. Mysels. Flow of thickened fluids, 1949. US Patent 2,492,173.

[54] R. Nagarajan. Molecular packing parameter and surfactant self-assembly: the neglected role of the surfactant tail†. *Langmuir*, 18(1):31–38, jan 2002.

[55] R. Nagarajan and E. Ruckenstein. Theory of surfactant self-assembly: a predictive molecular thermodynamic approach. *Langmuir*, 7(12):2934–2969, dec 1991.

[56] R. Oda, Janaky Narayanan, P. A. Hassan, C. Manohar, R. A. Salkar, F. Kern, and S. J. Candau. Effect of the lipophilicity of the counterion on the viscoelasticity of micellar solutions of cationic surfactants. *Langmuir*, 14(16):4364–4372, aug 1998.

[57] Yunying Qi, Yasuo Kawaguchi, Richard N. Christensen, and Jacques L. Zakin. Enhancing heat transfer ability of drag reducing surfactant solutions with static mixers and honeycombs. *International Journal of Heat and Mass Transfer*, 46(26):5161–5173, 2003.

[58] Yunying Qi, Yasuo Kawaguchi, Zhiqing Lin, Mark Ewing, Richard N Christensen, and Jacques L Zakin. Enhanced heat transfer of drag reducing surfactant solutions with fluted tube-in-tube heat exchanger. *International Journal of Heat and Mass Transfer*, 44(8):1495–1505, 2001.

[59] Yunying Qi, Kenneth Littrell, Pappannan Thiyagarajan, Yeshayahu Talmon, Judith Schmidt, Zhiqing Lin, and Jacques L. Zakin. Small-angle neutron scattering study of shearing effects on drag-reducing surfactant solutions. *Journal of Colloid and Interface Science*, 337(1):218–226, sep 2009.

[60] Yunying Qi, Linda K Weavers, and Jacques L Zakin. Enhancing heat-transfer ability of drag reducing surfactant solutions with ultrasonic energy. *Journal of Non-Newtonian Fluid Mechanics*, 116(1):71–93, 2003.

[61] Yitzhak Rabin and Barbara J. A. Zielinska. Scale-dependent enhancement and damping of vorticity disturbances by polymers in elongational flow. *Physical Review Letters*, 63(5):512–515, jul 1989.

[62] Takashi Saeki. Application of a drag reduction phenomenon caused by surfactant solutions. *J. Chem. Eng. Japan / JCEJ*, 47(2):175–179, 2014.

[63] R. H. J. Sellin, J. W. Hoyt, and O. Scrivener. The effect of drag-reducing additives on fluid flow and their industrial applications, part 1: basic aspects. *Journal of Hydraulic Research*, 20(1):29–68, 1982.

[64] Haifeng Shi, Wu Ge, Hyuntaek Oh, Sean M. Pattison, Jacob T. Huggins, Yeshayahu Talmon, David J. Hart, Srinivasa R. Raghavan, and Jacques L. Zakin. Photoreversible micellar solution as a smart drag-reducing fluid for use in district heating/cooling systems. *Langmuir*, 29(1):102–109, dec 2012.

[65] Haifeng Shi, Wu Ge, Hyuntaek Oh, Sean M. Pattison, Jacob T. Huggins, Yeshayahu Talmon, David J. Hart, Srinivasa R. Raghavan, and Jacques L. Zakin. Photoreversible micellar solution as a smart drag-reducing fluid for use in district heating/cooling systems. *Langmuir*, 29(1):102–109, 2013.

[66] Haifeng Shi, Wu Ge, Yi Wang, Bo Fang, Jacob T. Huggins, Tyler A. Russell, Yeshayahu Talmon, David J. Hart, and Jacques L. Zakin. A drag reducing surfactant threadlike micelle system with unusual rheological responses to pH. *Journal of Colloid and Interface Science*, 418:95–102, 2014.

[67] Haifeng Shi, Yi Wang, Wu Ge, Bo Fang, Jacob T. Huggins, Thaddaus R. Huber, and Jacques L. Zakin. Enhancing heat transfer of drag-reducing surfactant solution by an HEV static mixer with low pressure drop. *Advances in Mechanical Engineering*, 2011:1–10, 2011.

[68] Bryan C. Smith, Lu-Chien Chou, Bin Lu, and Jacques L. Zakin. Effect of counterion structure on flow birefringence and drag reduction behavior of quaternary ammonium salt cationic surfactants. In *ACS Symposium Series*, pages 370–379. American Chemical Society, dec 1994.

[69] R. E. Smith and W. G. Tiederman. The mechanism of polymer thread drag reduction. *Rheologica Acta*, 30(2):103–113, mar 1991.

[70] Marc C.A. Stuart and Egbert J. Boekema. Two distinct mechanisms of vesicle-to-micelle and micelle-to-vesicle transition are mediated by the packing parameter of phospholipid–detergent systems. *Biochimica et Biophysica Acta (BBA) - Biomembranes*, 1768(11):2681–2689, nov 2007.

[71] Hiroshi Suzuki, Gerald G. Fuller, Tomoe Nakayama, and Hiromoto Usui. Development characteristics of drag-reducing surfactant solution flow in a duct. *Rheologica Acta*, 43(3):232–239, 2004.

[72] Nguyen Anh Tuan and Hiroshi Mizunuma. Advection of shear-induced surfactant threads and turbulent drag reduction. *Journal of Rheology*, 57(6):1819–1832, nov 2013.

[73] M S Turner and M E Cates. Flow-induced phase transitions in rod-like micelles. *Journal of Physics: Condensed Matter*, 4(14):3719–3741, apr 1992.

[74] P. S. Virk. Drag reduction fundamentals. *AIChE J.*, 21(4):625–656, 1975.

[75] Myles Walsh. *On the turbulent flow of dilute polymer solutions*. PhD thesis, California Institute of Technology, 1967.

[76] Michael D. Warholic, Gavin M. Schmidt, and Thomas J. Hanratty. The influence of a drag-reducing surfactant on a turbulent velocity field. *Journal of Fluid Mechanics*, 388:1–20, 1999.

[77] J. L. Zakin, Y. Zhang, and W. Ge. Drag reduction by surfactant giant micelles. In Raoul Zana and Eric W. Kaler, editors, *Giant micelles: properties and applications*, page 473492. CRC Press LLC, 2007.

[78] Jacques L. Zakin, Bin Lu, and Hans-Werner Bewersdorff. Surfactant drag reduction. *Reviews in Chemical Engineering*, 14(4-5), 1998.

[79] R. Zana. Bolaform and dimeric (gemini) surfactants. In *Specialist Surfactants*, pages 81–103. Springer Netherlands, 1997.

[80] Raoul Zana. *Giant micelles : properties and applications*. CRC Press, Boca Raton, 2007.

[81] Ying Zhang, Judith Schmidt, Yeshayahu Talmon, and Jacques L. Zakin. Co-solvent effects on drag reduction, rheological properties and micelle microstructures of cationic surfactants. *Journal of Colloid and Interface Science*, 286(2):696–709, jun 2005.

[82] Y. Zheng. *Cryo-electron microscopy of microstructures in self-assembled colloidal systems*. PhD thesis, University of Minnesota, 2000.

[83] Yi Zheng, Z. Lin, J. L. Zakin, Y. Talmon, H. T. Davis, and L. E. Scriven. Cryo-TEM imaging the flow-induced transition from vesicles to threadlike micelles. *The Journal of Physical Chemistry B*, 104(22):5263–5271, jun 2000.